

Carbon soil stock change in an intensive crop field near Paris reveals significant carbon losses over a decade

Benjamin Loubet^{1*}, Nicolas P.A. Saby², Bruna Winck^{1,2}, Maryam Gebleh^{1,2}, Pauline Buysse^{1,3}, Jean-Philippe Chenu², Céline Ratié², Claudy Jolivet², Carmen Kalalian¹, Florent Levavasseur¹, Jose-Luis Munera-Echeverri², Sébastien Lafont⁴, Denis Loustau⁴, Dario Papale^{5,6}, Giacomo Nicolini⁷, and Dominique Arrouays^{2 †}

¹ ECOSYS, University Paris-Saclay, INRAE, AgroParisTech, Palaiseau, France

² Info&Sols, INRAE, Orléans, France

³ SAS, INRAE, Institut Agro Rennes-Angers, Rennes, France

⁴ Bordeaux Sciences-Agro, INRAE, ISPA, F-33610, Villenave d'Ornon, France

⁵ CNR IRET, Monterotondo Scalo, Italy

⁶ University of Tuscia, DIBAF, Viterbo, Italy

⁷ CMCC Foundation - Euro-Mediterranean Center on Climate Change, Viterbo, Italy

† deceased

* corresponding author: benjamin.loubet@inrae.fr

Abstract. Soil is a large pool of carbon (C), storing globally twice **as much** carbon **as** the atmosphere and **three times as much as** vegetation. Soil organic carbon (SOC) stocks are significantly impacted by land-use changes, either negatively when **forests** or grasslands are **converted** into crops or positively when the opposite **occurs**. This context underpins the “4per1000” initiative, which aims to promote SOC storage in soils as a mitigation strategy. However, intensive cropping and climate change may lead to **losses of** organic and inorganic carbon from soils, which calls for long-term observations of soil organic carbon stocks in reference ecosystems **worldwide**. To address this, a harmonised reference soil sampling protocol was developed for all ecosystem sites within the European Integrated Carbon Observing System (ICOS) research infrastructure, starting in 2017 with revisits planned every 5–10 years. This study presents a first case at the French cropland site FR-Gri (wheat–maize–barley–oilseed rape rotation), assessing SOC stock in 2019 with the ICOS protocol, which was combined with earlier SOC stock sampling data from the European project CarboEurope. A significant soil decompaction was observed over the 13.5 years **in the 0–30 cm layer**. Bulk density decreased by 22% in the 0–5 cm layer (from 1.31 to 1.02 g cm⁻³) and by 5% in the 5–30 cm layer (from 1.53 to 1.45 g cm⁻³), likely due to the adoption of reduced tillage since 2004. SOC content increased by 10% in the 0–5 cm layer but declined **by 6.2%** in the 5–30 cm layer. The SOC stocks based on equivalent soil mass (ESM) increased by 7.6% in the 0–5 cm layer, but decreased by 11% and 9% in the 5–30 **cm** and 30–60 cm layers, **respectively**. Overall, the ESM-based SOC stock in the 0–60 cm layer decreased by approximately 0.95 ± 0.22 kg C m⁻² (or 9 Mg C ha⁻¹) between 2005 and 2019, corresponding to **0.65% yr⁻¹ relative to the initial SOC stock (~11 kg C m⁻² in the 0–60 cm layer)**. This leads to an average **yearly** decrease rate of 0.072 ± 0.017 kg C m⁻² yr⁻¹ (or 0.72 ± 0.17 Mg C ha⁻¹ **yr⁻¹**), consistent with previous studies. To further interpret this trend, we applied the soil carbon cycling model AMG to simulate **soil carbon** dynamics down to a 30 cm depth from 2005 onwards. Based on site-specific exports and imports and estimated residue returns, the model predicted a SOC stock decline larger than the **observed one in the 0–30 cm depth, stabilising around 2028, assuming management stays the same in the future**. By 2040, SOC stocks are projected to decline to 6.9 kg C m⁻², representing an approximate 15% reduction from the 2005 baseline. Furthermore, the AMG simulation was also consistent with the carbon flux balance reported by Loubet et al. (2011) **for the period between 2006 and 2010**.

41 **The observed decrease in SOC stocks may be attributed to a shift towards larger exports, lower residue returns,**
42 **and reduced carbon imports** at this site compared to past management practices. This **study highlights the im-**
43 **portance of** high-quality SOC stock change monitoring, as developed **within** the ICOS research infrastructure.

44 **1 Introduction**

45 Soil is **one of the largest reservoirs of** carbon (C) and nitrogen (N) **in the terrestrial biosphere. Globally,** soils
46 store **approximately 1500- 2400 Gt of organic C (SOC) in the upper meter** (Batjes, 1996; Sanderman et al.,
47 2017) and **a comparable** amount as inorganic C to a depth of 2 m (Zamanian et al., 2021), **far exceeding the**
48 **carbon stored in the** atmosphere and vegetation **combined** (Antón et al., 2021). Hence, minor changes in **SOC**
49 **stocks can have substantial impacts on** atmospheric carbon dioxide (CO₂) concentrations **and climate feed-**
50 **backs** (Minasny et al., 2017).

51 **Agricultural management is a major driver of SOC dynamics through its control of organic matter inputs,**
52 **soil disturbance, and residue incorporation, in interaction with climate and soil properties (Paustian et al.,**
53 **2016). Intensive farming practices, such as simplified crop rotations, frequent tillage, and high fertiliser use,**
54 **have commonly been associated with SOC losses by accelerating organic matter decomposition and reduc-**
55 **ing C inputs to soils (Autret et al., 2016; Schmidt et al., 2011; Six et al., 2002). Conversely, management**
56 **practices that enhance C inputs (mineral fertilisation, diversified crop rotation, cover crops, organic amend-**
57 **ments) and reduce soil disturbance (reduced-tillage and no-tillage) have been shown to promote SOC accu-**
58 **umulation or slow SOC losses (Lal, 2004; Poeplau and Don, 2015; Schmidt et al., 2011). Based on a review**
59 **of practices, it has been hypothesised that generalising C-storing practices could increase C sequestration**
60 **in the upper metre of agricultural soils by 2 to 3 Pg C yr⁻¹, which roughly corresponds to 4 per 1000 per**
61 **year of the current C stock (Minasny et al., 2017). However, such estimates remain highly uncertain and**
62 **variable in space, while major concerns remain on the persistence of soil carbon gains over time as soils**
63 **approach a new equilibrium (Baveye et al., 2018; Franzluebbers et al., 2012).**

64 **In Europe, current bottom-up inventories show croplands as a net C source of 10 ± 9 g C m⁻² yr⁻¹, whereas**
65 **grasslands and forests act as net C sinks of 57 ± 34 g C m⁻² yr⁻¹ and 20 ± 12 g C m⁻² yr⁻¹, respectively (Schrumpf**
66 **et al., 2011; Schulze et al., 2009). However, top-down estimates of terrestrial C budgets indicate that European**
67 **terrestrial ecosystems are an overall sink of approximately -100 Tg C yr⁻¹, but with considerable associated**
68 **uncertainties of ±360 Tg C yr⁻¹ (Petrescu et al., 2021). Accurately quantifying temporal changes in SOC stocks**
69 **remains a significant source of uncertainty in terrestrial carbon budgets.**

70 **Reliable** monitoring of SOC stocks **requires** accurate quantification of the **bulk density (BD)**, the fine earth
71 fraction (**FE, the fraction of soil below 2 mm**), and the **carbon content, throughout the soil profile** (Molteni
72 and Corti, 1998), **as well as a sufficiently dense sampling design** to reduce uncertainty **associated with spatial**
73 **variability** (Batjes, 1996). Bulk density **measurements are** often **complex and time-consuming, particularly**
74 **in rocky soils, and are therefore frequently estimated using pedotransfer functions (PTFs). However, the**
75 **use of PTF-derived BD** can introduce systematic bias, **particularly when rock fragments (RF) are inade-**
76 **quately accounted for, or when circular predictors such as SOC content are used** (Schrumpf et al., 2011; Xu
77 et al., 2015). **But bulk density can substantially vary over decades, in response to management practices, soil**
78 **compaction and decompaction, erosion, and climate-driven soil processes such as wetting–drying cycles,**

79 **freeze–thaw dynamics, and shrink–swell behaviour of clay soils** (Hopkins et al., 2009). **Because BD directly**
80 **determines soil mass, such variations critically affect estimates of SOC stock over time.**

81 To address this issue, Ellert and Bettany (1995) proposed the equivalent soil mass (ESM) method **as an alternative**
82 **to** the fixed depth (FD) method **for measuring** SOC stock changes. In the FD method, SOC stock changes are
83 evaluated at constant soil depths and can induce significant biases **when BD varies over time** (Beem-Miller et al.,
84 2016). In the ESM approach, SOC stocks are evaluated for a constant soil mass per unit area, thereby compensating
85 for changes in BD by adjusting the soil depth accordingly (Ellert and Bettany, 1995; von Haden et al., 2020;
86 VandenBygaart and Angers, 2006; Wendt and Hauser, 2013). Differences between FD and ESM can **account for**
87 **up to 10% of SOC changes and may** overwhelm variations caused by tillage and crop residue removal rates (Du
88 et al., 2017; Xiao et al., 2020). As comparing SOC stocks on the same soil mass per unit area is recognised as a
89 better practice than the FD approach, this methodology was included as the reference method by FAO and IPCC
90 (FAO, 2019; IPCC, 2019).

91 Soil organic **C** stocks are key **estimates within** the Integrated Carbon Observation System (**ICOS**), a European
92 Research Infrastructure Consortium (Heiskanen et al., 2022). As of 2025, ICOS **includes** 45 high-quality and
93 standardised ecosystem sites (Class 1 and 2 stations), covering the diversity of European soils and ecosystems.
94 **Within ICOS, SOC stocks have been** measured **since 2017** and **will be re-measured every** 10 years **to quantify**
95 **changes in SOC stock over time. To ensure unbiased and robust estimates with a limited number of samples**
96 **(Arrouays et al., 2018; Don et al., 2007; Saby et al., 2008), ICOS adopts a Design-Based (DB) approach**
97 **(Brown, 1992; Collins, 1992) with randomly selected sampling points (Arrouays et al., 2018; Brus and**
98 **deGruijter, 1997; de Gruijter et al., 2006; Loustau et al., 2017). At each ICOS site, the measured soil** stock
99 change over time can then be compared to the integrated **CO₂** fluxes at the site boundaries over that period, which
100 comprise the net ecosystem productivity, imports to and exports from the site, and lixiviated fluxes (Aubinet et al.,
101 2009; Ceschia et al., 2010; Loubet et al., 2011). Soil carbon cycling models such as DAYCENT (Parton et al.,
102 1998), **STICS** (Brisson et al., 1998), RothC (Coleman and Jenkinson, 1996), or AMG (Clivot et al., 2019) are
103 essential tools to further understand the observed SOC dynamics based on site-specific managements, and in par-
104 ticular exports, imports, and residue returns. Models are also key in providing long-term simulation of SOC stock
105 dynamics and scenario analysis.

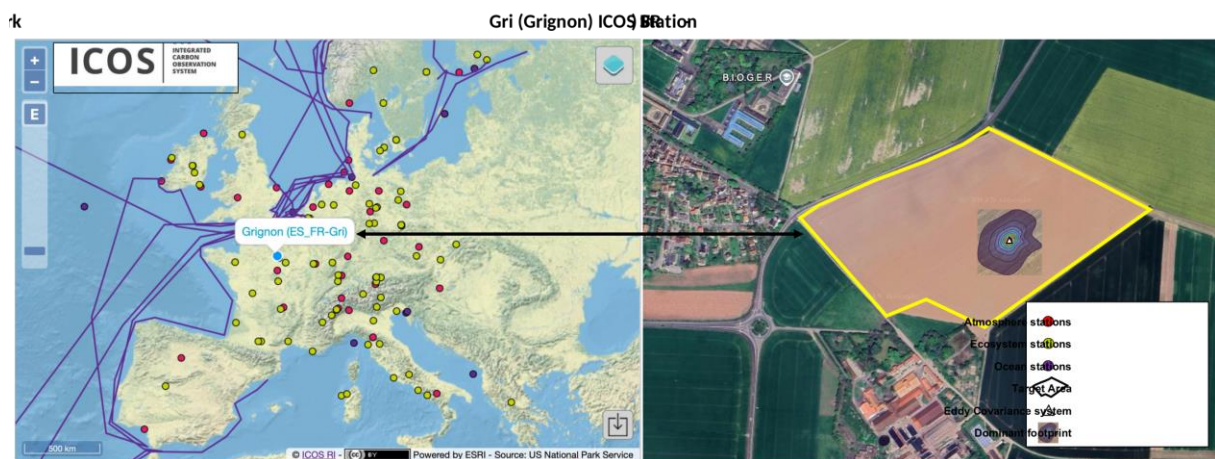
106 **Given** the 10-year **resampling** interval, evaluations **of SOC stock changes, entirely based on** the ICOS **protocol,**
107 will only **become** available **starting in 2027**. However, **before ICOS, several European** sites were sampled from
108 2005 to 2010 using a systematic grid-based sampling **design** within the EU CarboEurope project (**Schrumpf et**
109 **al., 2011), providing a unique opportunity to assess SOC stock changes, while explicitly addressing method-**
110 **ological challenges related to sampling design, bulk density variability, and SOC stock calculation ap-**
111 **proaches.** At the Grignon **ICOS ecosystem** station (FR-Gri), a cropland site, SOC **stock** was measured in 2005
112 using **a** grid-based design and **later** in 2019, using the ICOS protocol. The objectives of this study are to (1)
113 **quantify** SOC stock change between 2005 and 2019 at **the** FR-Gri station, (2) compare **SOC stock changes**
114 **estimates obtained using** the equivalent soil mass and fixed depth **approaches,** (3) discuss the uncertainties **re-**
115 **lated to** these estimations, **mainly those related to sampling design,** and (4) compare the **observed SOC stock**
116 **changes with predictions from the AMG** soil carbon model (Clivot et al., 2019) and **with** previously established
117 carbon flux balance estimations at the same site by Loubet et al. (2011).

118 **2 Materials and methods**

119 **2.1 Study site**

120 The study was conducted at the Grignon station, an ICOS ecosystem site (ICOS code FR-Gri, class 2 since 2021).
121 It is a crop field of 19 ha located 40 km west of Paris, in northern France (48.9°N, 1.95°E; elevation 125 m) (**Figure**
122 **1**). During the **study period** (2005-2019), the mean annual air temperature and rainfall were 11.2 °C and 586 mm,
123 respectively. The site has a gentle north-eastward slope of approximately 1%. Agricultural fields mostly surround
124 the south and west of the study area. The surface soil (0–15 cm layer) is classified as silt loam, with a particle-size
125 distribution of 98 g kg⁻¹ sand, 713 g kg⁻¹ silt, and 189 g kg⁻¹ clay. The effective soil depth (A + B horizons) varies
126 from approximately 0.4 m in the north-east to over 1 m in the south-west. Soils across the parcel exhibit calcic
127 horizons, with average CaCO₃ contents of 3% in the 0–50 cm layer and 20% in the 50–100 cm layer, and an
128 alkaline soil pH of 7.6. (**Table S1**). The OC content in the surface layers was around 20 g C kg⁻¹ as reported in
129 2011 (Loubet et al., 2011).

130



131

132 **Figure 1. (A) Map of the ICOS station network across Europe, showing atmosphere (red), ecosystem (green), and ocean**
133 **(blue) stations. The Grignon site (FR-Gri) is highlighted. (B) The 19-ha field site at FR-Gri, shown in a Google Maps**
134 **image, with the target area outlined in yellow. The eddy covariance system (white triangle) is located centrally, sur-**
135 **rounded by its dominant flux footprint (shaded gradient area). The site, with a mixed farm with cattle and sheep housed**
136 **in the southern buildings, has been cultivated for over 100 years, although the exact start year is unknown. The site is**
137 **highly fertilised with sewage sludge in the 1980s.**

138

139 In 2004, as part of **implementing** reduced tillage **in** the crop rotation system, the soil was scarified to a depth of
140 **50 cm** to reduce compaction. Since then, most tillage operations have been restricted to the superficial layer (0–
141 **15 cm**), using a stubble cultivator or a clod crusher. Two additional scarification events were carried out: one in
142 2010 (to a depth of 25 cm) and another in 2012 (to a depth of 40 cm). Additionally, the soil is disturbed to a depth
143 of 5 or 10 cm during seeding operations.

144

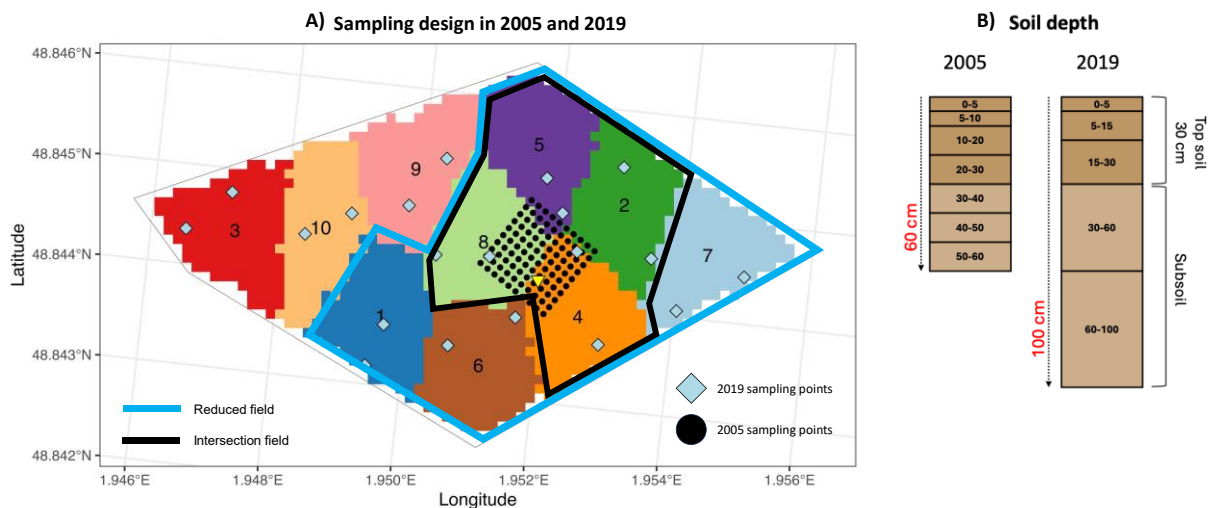
Table 1. Crop rotation, yield, exports and imports, and nitrogen (N) applied over the 15 years between the two sampling campaigns at the FR-Gri site. Carbon export was evaluated based on the farmer's record of grain, straw, and silage exports. The aerial crop residue return was evaluated based on the exports and the allometric coefficient of the AMG model, as explained in the manuscript. A 0.44 g C g⁻¹ dry biomass carbon content was assumed to compute the exports and imports. Organic nitrogen was mainly cattle slurry and, on a few occasions, manure. Mineral fertilisation was mainly urea-ammonium-nitrate.

crop	year	part of the plant harvested	Exported Carbon (g C m ⁻²)	Imported Carbon (g C m ⁻²)	Aerial Crop Residues returned to the soil (g C m ⁻²)	Organic Nitrogen applied (kg N ha ⁻¹)	Mineral Nitrogen applied (kg N ha ⁻¹)	Total Nitrogen applied (kg N ha ⁻¹)
mustard	2005	None			90 ± 10			
maize	2005	above 20 cm -	330 ± 40		10 ± 0		140 ± 10	140 ± 10
wheat	2006	seed and straw	640 ± 70		170 ± 20		110 ± 10	110 ± 10
barley	2007	seed and straw	440 ± 50		150 ± 20		110 ± 10	110 ± 10
mustard	2008	None			90 ± 10			
maize	2008	above 20 cm -	550 ± 60	120 ± 20	20 ± 0	80 ± 10	60 ± 0	130 ± 10
wheat	2009	seed, straw, and chaff	640 ± 70	140 ± 20	150 ± 10	80 ± 10	170 ± 10	250 ± 20
Triticale	2010	seed, straw, and chaff	490 ± 60	240 ± 40	90 ± 10	220 ± 40	100 ± 10	320 ± 40
maize	2011	above 20 cm -	610 ± 70	120 ± 20	20 ± 0	80 ± 10		80 ± 10
wheat	2012	seed, straw, and chaff	640 ± 70	160 ± 30	100 ± 10	170 ± 30	70 ± 0	240 ± 30
rapeseed	2013	seed and chaff	240 ± 30		370 ± 40		110 ± 10	110 ± 10
wheat	2014	seed and straw	420 ± 50	180 ± 30	110 ± 10	130 ± 20	110 ± 10	240 ± 20
mustard	2015	None			90 ± 10			
maize	2015	above 20 cm -	430 ± 50	280 ± 50	20 ± 0	290 ± 50		290 ± 50
wheat	2016	seed, straw, and chaff	440 ± 50	50 ± 10	190 ± 20	90 ± 20	220 ± 10	310 ± 20
rapeseed	2017	seed	170 ± 20		440 ± 40	0 ± 0	120 ± 10	120 ± 10
wheat	2018	seed and straw	450 ± 50	300 ± 50	130 ± 10	190 ± 30	80 ± 0	270 ± 30
mix intercrop	2019	All plants for silage	50 ± 10				40 ± 0	40 ± 0
maize	2019	above 20 cm -	540 ± 60	120 ± 20	20 ± 0	80 ± 10		150 ± 10
		average (g C m ⁻² y ⁻¹ or kg N ha ⁻¹)	470 ± 54	114 ± 13	151 ± 17	93 ± 11	100 ± 11	193 ± 22

150 The crops in the rotation system are winter wheat, silage maize (preceded by a mustard catch crop), and winter
151 barley, with two years of oilseed rape during the period (Table 1). These crops are herbaceous, with C3 (wheat,
152 barley, triticale, oilseed rape, mustard) or C4 (maize) plants. Crop production is primarily exported as grain or
153 silage (maize), but residues are also exported for use as animal feed and for bioenergy purposes. The average
154 carbon export was $470 \pm 54 \text{ g C m}^{-2} \text{ yr}^{-1}$ (Table 1). The field received regular applications of slurry and manure,
155 with an average carbon input of $114 \pm 13 \text{ g C m}^{-2} \text{ yr}^{-1}$. The average above-ground biomass crop residues left on
156 the field were evaluated using the exported biomass and allometric coefficients (Clivot et al., 2019). They represent
157 $151 \pm 17 \text{ g C m}^{-2} \text{ yr}^{-1}$, approximately one-third of the exported carbon, which is slightly higher than the amount
158 imported. The biomass of mustard was not measured but taken equal to the mean estimated biomass of mustard in
159 France, -2 Mg DM ha^{-1} (Soleilhavoup and Crisan, 2021).

161 2.2 Soil sampling schemes

162 The two campaigns were conducted in different areas around the eddy covariance system. The 2005 campaign
163 focused on an area representative of the eddy covariance mast's maximum footprint, while the 2019 campaign
164 encompassed the entire 19 ha field. The footprint determined using the Kljun approach (Kljun et al., 2004, 2015)
165 was well within the 19-ha field (Figure 1), except on some stable nights when it extended into the surrounding
166 area. Two different soil sampling strategies were employed during the 2005 and 2019 campaigns (Figure 2). In
167 the 2005 campaign, 100 soil cores were taken using a systematic sampling grid ($7 \times 7 \text{ m}$), and samples were
168 collected with both 8.3 cm and 8.7 cm inner diameter corers in December 2005, during the winter wheat dormancy
169 period. Soil cores were divided into seven layers (0-5, 5-10, 10-20, 20-30, 30-40, 40-50, and 50-60 cm). The 2005
170 campaign results were reported in Schrumpf et al. (2011). In the 2019 campaign, 99 soil samples (20 locations \times
171 5 depths - 1) were collected in March, following the ICOS protocol (Arrouays et al., 2018; Loustau et al., 2017),
172 which consists of a stratified simple random sampling design. One sample, located between 60 and 100 cm, was
173 not reachable due to the high rock density. The field was at that time covered with a mix of catch crops (oats, field
174 bean, pea, clover, and flax). The studied area was divided into 10 geographically compact equal-area strata (Wal-
175 voort et al., 2010). Within each stratum, two primary sampling points (SP-I) were randomly selected (simple ran-
176 dom) for a total of 20 SP-I plots. At each SP-I, five secondary sampling points (SP-II) were randomly selected
177 within a buffer area of 10 meters, where the soil was sampled using a 5.5 cm inner diameter corer. Each core was
178 separated into subsamples at depths of 0-5 cm, 5-15 cm, 15-30 cm, 30-60 cm, and 60-100 cm. Finally, cores
179 were mixed to form a composite sample at each primary location and each layer. The spatial stratification and
180 sampling point distribution were performed using the R package "spcosa" (Walvoort et al., 2010). To ensure
181 comparability between the 2005 and 2019 sampling campaigns, all SOC stock change analyses presented in
182 this study were restricted to a spatially comparable subset of the field, which exhibited similar pedological
183 properties in 2005 and 2019 (Figure S4). A detailed spatial comparison between the two sampling cam-
184 paigns, including clustering analyses and sensitivity tests across different spatial subsets, is provided in the
185 Supplementary Material (Figure S1-S5).



187
 188 **Figure 2. A) Map of the study area showing the spatial distribution of sampling zones and soil core depth segmentation.**
 189 **Soil sampling was conducted at two times: in 2005 (black circles) and 2019 (blue diamonds). For the 2019 sampling, the**
 190 **field was stratified into 10 strata (coloured polygons, labelled 1–10), and the sampling points were randomly located**
 191 **within each stratum. The 2005 sampling followed a grid-based sampling design that partially covered strata 2, 4, 5, and**
 192 **8, with the majority of the sampling concentrated in strata 8 and 4. Blue polygon represents the “Reduced field” and**
 193 **black polygon the “Intersection field”. B) Segmentation of soil cores into depth intervals for two different sampling**
 194 **protocols: 60 cm cores (six layers: 0–5, 5–10, 10–20, 20–30, 30–40, and 50–60 cm) and 100 cm cores (five layers: 0–5, 5–**
 195 **15, 15–30, 30–60, and 60–100 cm). Latitude and longitude are shown in WGS 84 coordinates.**

196
 197 **2.3 Soil samples preparation and analyses**

198 In the 2005 campaign, all soil samples were preserved at 4°C before processing. The coarse fraction – rock (RF)
 199 ($\emptyset > 4$ mm) and root fractions ($\emptyset > 1$ mm) - were separated from the samples and subsequently air-dried at 40°C.
 200 The remaining samples were sieved to < 2 mm to obtain the fine earth (FE) fraction and the coarse fraction (> 2
 201 mm). Subsequently, each fraction was weighted (Schumpf et al., 2011). In the 2019 campaign, samples from SP-
 202 II plots were air-dried at 30°C and then sieved to separate the FE fraction (< 2 mm). The root and rock fractions
 203 were oven-dried at 70°C and 105°C, respectively, before weighing. Subsequently, the FE fraction from each depth
 204 interval of the five SP-II plots was proportionally mixed (based on the weight contribution of each layer) to create
 205 a composite sample (SP-I). The BD, residual water and FE fraction were computed from the SP-II samples, then
 206 averaged at the SP-I level, and the C content was measured on the SP-I composite samples. See Arrouays et al.
 207 (2018) and ICOS protocol (Loustau et al. 2017) for more information. In both campaigns, the FE fraction was then
 208 split into three subsamples to measure the C content (air-dried sample), residual water (after drying at 105°C) and
 209 soil bulk density (BD). Soil organic carbon (SOC) content ($C, \text{g kg}^{-1}$) was determined in the air-dried FE fraction
 210 by dry combustion (ISO 10694), which measures the total carbon content in the soil. Overall, the soil preparation
 211 and analysis **methods used in 2005 and 2019** were very similar. Carbonate ($\text{CaCO}_3, \text{g kg}^{-1}$) was measured by
 212 determining the loss of carbon dioxide (CO_2) after acidification with hydrochloric acid in 2019. The inorganic
 213 carbon content was also determined in 2019: when CaCO_3 content was lower than 700 g kg^{-1} , the soil inorganic
 214 carbon (SIC) content was calculated as $C = 0.12 \times \text{CaCO}_3$. When **the** CaCO_3 content exceeded 700 g kg^{-1} , to avoid
 215 a deterioration in the accuracy of organic carbon deduced from total carbon, samples were first treated with HCl
 216 to eliminate carbonates, and then total carbon was determined as previously **explained**. The SOC content was then
 217 computed as the total carbon content minus the inorganic carbon content.

218 2.4 Soil data pre-processing

219 **Before** statistical analysis, missing values in the 2005 dataset were imputed using Ordinary Kriging interpolation
220 (Goovaerts, 1997), which leverages spatial autocorrelation to provide unbiased and minimum variance estimates
221 of missing data points. Using spatial coordinates, the target variables were estimated based on interpolated values
222 derived from a fitted variogram model (Nugget + Spherical) and up to 35 neighbouring data points within a 100-
223 unit radius. For the 2019 dataset, which had only a single missing value, we used the average value of the corre-
224 sponding soil layer.

225 2.5 Soil carbon stocks calculation using the fixed-depth (FD) approach

226 The soil carbon stock SOC_{stock} (kg C m⁻²) across the soil layers was calculated following Poeplau et al. (2017):
227

$$228 \quad SOC_{stock} = \sum_{i=1}^n \frac{m_{FE_i}}{m_{soil_i}} \times BD_i \times \Delta z_i \times SOC_i \times \frac{1}{1000} \times 10000 \quad (1)$$

229
230 Where n is the number of layers in which the soil core was divided down to 60 cm, i is the layer index, m_{FE_i} (g)
231 is the mass of fine earth in the layer, and m_{soil_i} (g) is the total soil mass of the layer (including rocks and roots),
232 BD_i (g cm⁻³) is the bulk density of the layer, Δz_i is the layer thickness (cm), and SOC_i (g C kg⁻¹) is the SOC content
233 in the FE fraction in the layer. The factor **of** $\frac{1}{1000}$ converts SOC content from g kg⁻¹ to kg kg⁻¹, and the factor **of**
234 10000 converts cm² to m². The bulk density in each soil layer is defined as the ratio of m_{soil_i} to the soil core
235 volume V_{sample_i} :

$$236 \quad BD_i = \frac{m_{soil_i}}{V_{sample_i}} = \frac{m_{soil_i}}{S_i \times \Delta z_i} \quad (2)$$

238
239 where S_i is the sampled surface. Equations (1) and (2) correspond to equations (1) and (2) in Schrumpf et al. (2011)
240 and were used to compute the stocks for the 2005 samples. We note that when combining equations (1) and (2),
241 the mass of soil m_{soil_i} and the layer thickness Δz_i disappear. In the ICOS stock calculation protocol, the bulk
242 density is therefore **no longer** used. The SOC stocks are computed based on the surface sampled S_i and the mass
243 of fine earth m_{FE_i} only. By further simplifying the **conversion** factors, one gets:

$$244 \quad SOC_{stock} = \sum_{i=1}^n \frac{m_{FE_i}}{S_i} \times SOC_i \times 10 \quad (3)$$

246
247 In equation (3), a term can be identified as the fine earth in each layer, $FE_i = m_{FE_i}/S_i \times 10$ (kg m⁻²), which gives
248 the fine earth over the 0-60 cm profile:

$$249 \quad FE_{60cm} = \sum_{i=1}^n \frac{m_{FE_i}}{S_i} \times 10 = \sum_{i=1}^n FE_i \quad (4)$$

251
252 We note here that these equations are adapted for core sampling. When sampling soils with pits, some corrections
253 need to be introduced in equations (1-3) to account for large stones and large roots in the pit. The inorganic carbon

254 stock SIC_{stock} is computed in a similar way as the SOC_{stock} but replacing the OC content in the FE fraction SOC_i
 255 by the inorganic carbon content SIC_i . Finally, the cumulative $SOC_{stock}^{0-60\text{ cm}}$ was computed after summing the stocks
 256 per layer.

257 2.6 Harmonisation of soil layers in both sampling campaigns

258 To ensure comparability between campaigns, the soil sampling depth (**Figure 2**) of each campaign was harmonised
 259 into three coarser layers: 0–5 cm, 5–30 cm, and 30–60 cm. Bulk density, rock fragments, and carbon content were
 260 aggregated using a thickness-weighted mean to account for variable layer depths, while SOC stocks and fine earth
 261 mass were calculated as cumulative sums across the respective layers. **All subsequent SOC stock calculations**
 262 **and statistical analyses were performed on these layers. Additional layers are provided in the supplemen-**
 263 **tary material.**

264 2.7 Soil carbon stocks calculation using the equivalent soil mass (ESM) and SOC stocks changes

265 To properly estimate SOC stocks evolution, one needs to consider changes in SOC content of the soil (SOC) but
 266 also the potential changes in BD_i due to compaction or decompaction, which may change the fine earth mass FE_i
 267 in each sampling depth (Lipiec and Hatano, 2003). Additionally, soil erosion driven by rainfall or wind can export
 268 soil particles – mainly silt and clay - out of the field. Erosion is thought to be negligible at the FR-Gri site due to
 269 a slight slope and systematic winter inter-cropping. Decompaction may have happened since the site was converted
 270 to reduced tillage from 2000 onwards (Loubet et al., 2011), but compaction in subsoil may also occur due to
 271 repeated surface traffic by heavy machinery (Liebhard et al., 2025; Lu et al., 2021). To consider possible changes
 272 in BD_i , the SOC stock evolution was estimated using the equivalent soil mass method (ESM), where the SOC
 273 stock is integrated down to a varying depth corresponding to a reference soil mass that is set equal for each cam-
 274 paign (Ellert and Bettany, 1995; von Haden et al., 2020; Lee et al., 2009; Wendt and Hauser, 2013). This approach
 275 has the advantage of accounting for a common sampling bias **associated** with the hydraulic corer, **namely** soil
 276 compaction.

277 The ESM-based SOC stock was computed using the R function “*SimpleESM*” (Ferchaud et al., 2023), which im-
 278 plements the classical ESM method (Ellert and Bettany, 1995) and ESM2, a model-based approach incorporating
 279 cubic splines (Wendt and Hauser, 2013). The reference fine earth mass (FE_{ref}) was derived from the median
 280 values in the 2005 dataset for the aggregated soil layers: 0–5 cm, 5–30 cm, and 30–60 cm (**Table 1**). The total FE
 281 in the 0–60 cm layer ranged from 852 to 967 kg m⁻² in 2005, and from 831 to 953 kg m⁻² in 2019 (**Table S4**).
 282

283 **Table 2. Reference fine earth mass (FE_{ref}) per layer used in the equivalent soil mass approach (ESM).**

Layer	Upper depth		Lower depth	FE_{ref} kg m ⁻²
	cm			
L1	0		5	63.2
L2	5		30	372.6
L3	30		60	453.1

284
 285 In the “classical” ESM approach (Ellert and Bettany, 1995), SOC stock is calculated by 1 mm increments (Autret
 286 et al., 2016; Mary et al., 2020). In brief, soil depth is discretised into elementary layers of 1 mm thickness, with
 287 FE density (g cm⁻³) and carbon content (g kg⁻¹) assigned to each 1 mm layer. Since both FE density and the SOC
 288 content are typically reported as average values over macro-layers (e.g., 0–5 cm), these values are assumed to be

289 constant within each 1 mm sublayer. Subsequently, FE_i and SOC_{stock_i} are then computed cumulatively until the
 290 FE_{ref} is reached. This approach is referred to as “*ESM non model*” by Peng et al. (2024). The ESM2 approach is
 291 based on the "material coordinate system" (Lee et al., 2009; McBratney and Minasny, 2010) or the "cumulative
 292 coordinates approach" (Rovira et al., 2015). This method uses a *post-hoc* model - a cubic spline interpolation - to
 293 mathematically adjust SOC measurements to a common fine earth mass (von Haden et al., 2020; Wendt and
 294 Hauser, 2013). As both **ESM and ESM2** methods yielded similar results (**Figure S6**), only ESM outcomes are
 295 reported in the following.

296 **2.8 Statistical inference for assessment of the carbon stock change**

297 Unequal variance t-tests (Welch’s t-test) were applied to assess significant differences between the two campaigns’
 298 means of SOC stocks estimated by FD and ESM approaches and other soil variables. The Welch’s t-test value was
 299 calculated as:

$$300 \quad t = \frac{(\widehat{X}_{2005} - \widehat{X}_{2019})}{\sqrt{\widehat{V}(\widehat{X}_{2005}) + \widehat{V}(\widehat{X}_{2019})}} \quad (5)$$

301 Where \widehat{X} is the estimated mean of the soil property X, $\widehat{V}(\widehat{X})$ is the estimated sampling variance of the estimated
 302 mean, and indexes stand for the campaign years. A design-based approach was used to estimate the means and
 303 sampling variances (de Gruijter et al., 2006). The sampling variances of the two campaigns were estimated sepa-
 304 rately and considered unequal. For the 2019 campaign, a stratified random sampling **method** with equal-area
 305 strata was **employed**. With the same number of sites per stratum, the mean and the sampling variance are estimated
 306 as:

$$307 \quad \widehat{X} = \frac{1}{N} \sum_{i=1}^N X_i \quad (6)$$

$$308 \quad \widehat{V}(\widehat{X}) = \sum_{h=1}^H w_h^2 \widehat{V}(\widehat{X}_h) = \frac{1}{4} \sum_{h=1}^H \widehat{V}(\widehat{X}_h) \quad (7)$$

309 Where X_i is the measured soil property at location i , N is the total number of samples over all strata, $\widehat{V}(\widehat{X}_h)$ is the
 310 sampling variance of stratum h , $w_h^2 = \frac{1}{4}$ is the weight of stratum h , and H is the number of strata.

311 For systematic random sampling (2005 campaign), the mean estimate is simple (Eq. 6), but there is no unbiased
 312 estimate of the sampling variance. We implemented the approximation suggested by Brus and Saby (2016), where
 313 the systematic random sample is treated as a stratified simple random sample. The sampling units were thus clus-
 314 tered by 2 based on their spatial coordinates into $H = n/2$ clusters ($n = 100$) using a k -means algorithm. The 2
 315 sampling units of a cluster were treated as a simple random sample from a stratum, and the variance was estimated
 316 with eq. (7) with $H = 50$. The weights were computed by $w_h^2 = n_h/n$, where $n_h = 2$ is the number of units per
 317 cluster. The 95% confidence interval is given by:

$$318 \quad \widehat{X} \pm t_{2.5}^{N-H} \sqrt{\widehat{V}(\widehat{X}_h)} \quad (8)$$

319 Where $t_{2.5}^{N-H}$ is the 2.5 quantile of a t distribution where $(N - H)$ approximates the degrees of freedom. For the
 320 2005 campaign, **the** degree of freedom **was** $N - H = 100 - 50 = 50$. In 2019, when the *Complete field* was
 321 considered, there were $H = 10$ strata of 2 units each, leading to a total number of sampling points $N = 20$ (called
 322 SP-I in ICOS), leading to $N - H = 10$. When part of the field was considered, both the number of samples and H
 323 diminished leading to $N - H < 10$. In 2005 and 2019, equations (7-9) **were** used to compute the carbon stock

324 statistics for each sampling depth available and over aggregated layers 0-15 cm, 15-30 cm and 30-60 cm. We also
325 computed the minimum detectable difference (MDD) based on a t-test with 95% confidence and 90% power ($\alpha =$
326 0.05 , $\beta = 0.10$).

327 Finally, we performed an additional statistical analysis to quantify the magnitude of SOC stock changes between
328 2005 and 2019 by calculating effect sizes using Hedges' g . This metric is a standardised mean difference method
329 that includes a correction for small sample sizes (Hedges, 1981), which was especially the case when using the
330 Reduced and Intersection fields, leading to 14 and 8 samples, respectively. Confidence intervals for effect-size
331 estimates were computed using 20000 nonparametric bootstraps with resampling and the bias-corrected and ac-
332 celerated (BCa) method (Canty et al., 2024; Efron, 1987; Kirby and Gerlanc, 2013). Negative values of Hedges'
333 g indicate a reduction in SOC stocks from 2005 to 2019, while positive values indicate an increase. If the confi-
334 dence intervals (CIs) include zero, it suggests that there is no significant difference in SOC stocks between the two
335 sampling years. These analyses were performed using the R package "bootES" (Kirby and Gerlanc, 2013).
336 See the equations (s1-s5) in the supplementary material.

337 2.9 Simulation of carbon stock evolution with the AMG model

338 We computed the SOC stock changes using the agricultural soil carbon model AMG (Clivot et al., 2019) to com-
339 pare with measured changes in SOC stock in the surface soil layer (0-30 cm). AMG is a relatively simple soil
340 carbon model that simulates SOC stocks by partitioning the soil carbon into three pools: (1) a pool receiving
341 organic C inputs from crop residues, roots, and exogenous organic matter (EOM), (2) an active organic C pool
342 subject to decomposition, and (3) a stable organic C pool. As stable C presents slow turnover, considering the
343 timescale of the simulation, **this pool is considered inert in the model and neither decomposes nor receives**
344 new C inputs.

345 A proportion (h_a) of **all the C inputs to the soil** is allocated to the active C pool, while the remaining proportion
346 ($1 - h_a$) is **considered** mineralised. The active C pool decomposes following first-order kinetics, with a rate con-
347 stant (k) that depends on climate variables (annual temperature, precipitation, **and** potential evapotranspiration)
348 and soil properties (clay content, carbonate content, pH, and C:N ratio). The C inputs to the soil include above-
349 ground crop residues and organic amendments from manure and slurry as listed in **Table 1**, plus the belowground
350 crop residues **and rhizodeposition** estimated from allometric equations based on the aboveground biomass (Clivot
351 et al., 2019, 2023). Roots and rhizodeposition C inputs down to a considered depth i are computed as:

$$352 C_{below\ ground\ inputs}(i) = \frac{DM_{AG}}{SRR} * 0.4 * 1.65 * (1 - \beta^i) \quad (9)$$

353 Where DM_{AG} is the **above-ground biomass**, SRR is the shoot-to-root-ratio, 0.4 is the carbon content of the roots
354 (40%), 1.65 is a factor accounting for the dead roots and rhizodeposition, assumed to be 65% of the living roots
355 C, and $(1 - \beta^i)$ accounts for the roots' distribution in the soil, where β is a crop-dependent parameter.

356 The SOC stock changes were simulated on an annual timestep over the period 2005–2040, considering the 0-30
357 cm depth layer, which generally corresponds to the managed soil layer in cropland systems, where most crop roots
358 and residue inputs occur. The baseline SOC stock **in the 0-30 cm layer** was set to 8.25 kg C m⁻², based on meas-
359 urements from 2005. The proportion of **the stable organic carbon pool** was set to 65% ($C_s = 0.65$), as **proposed**
360 **by** Clivot et al. (2019) for agricultural fields with a long-term history of cultivation. To assess model sensitivity,

we performed additional simulations **by** varying key management and environmental factors **and comparing to a base scenario**: (1) residue returns to the soil were increased to **100% of the available residues**, (2) organic amendments were either eliminated (set to zero) or doubled (multiplied by two), (3) meteorological conditions were **set to the pre-2005 period** by repeating the 1987–2004 weather data for the 2005–2040 period, and (4) the **proportion** of stable **organic carbon pool** (Cs) was **set to** 0.63 and 0.75 **as** independent estimates on a nearby soil reported by Kanari et al (2022) to illustrate the model’s response to this critical **soil carbon parameter**. **In the base scenario, (1) the residue returns and (2) the organic amendments were set according to Table 1, (3) the meteorological conditions were those measured at the site between 2005 and 2019, and then repeated to 2040, and (4) Cs was set to 0.65.**

2.10 Carbon flux balance derived from Eddy Covariance measurements

The carbon flux balance was estimated from 2006 to 2010 in Loubet et al. (2011), based on the Eddy Covariance (EC) micrometeorological method. The net biome productivity (NBP), representing the carbon balance of the field, was computed as:

$$NBP = NEE + F_{orga.fert} + F_{seeds} - F_{leach} - F_{harvest} \quad (10)$$

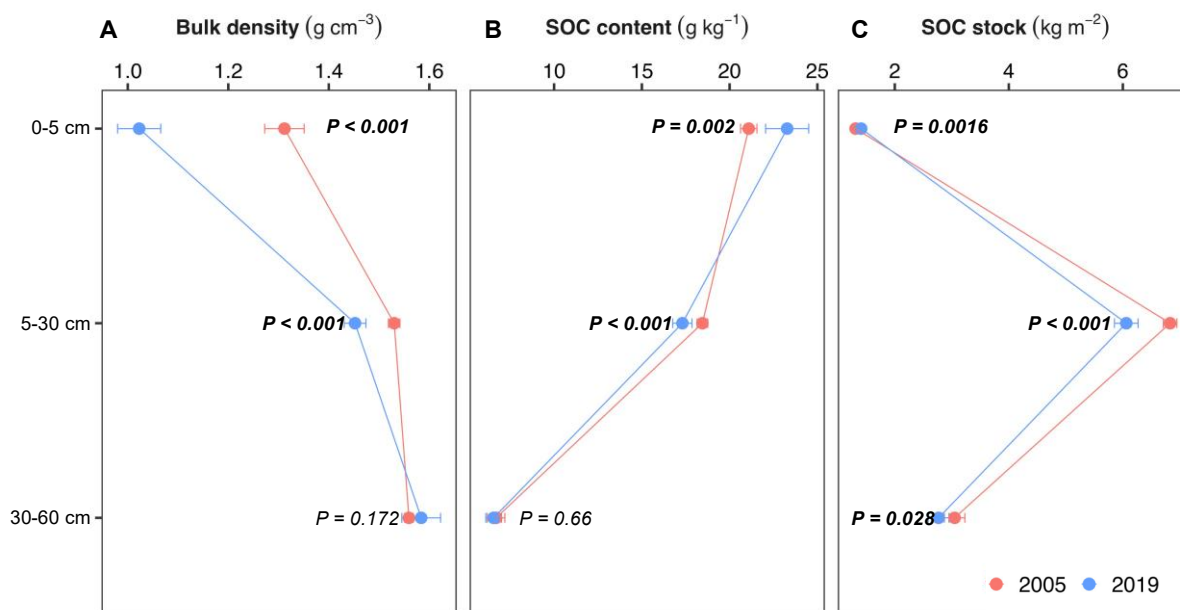
where NEE is the net ecosystem exchange of CO_2 flux over time, $F_{orga.fert}$ is the carbon input through organic fertilisation, F_{seeds} is the carbon input through seedling, F_{leach} is the organic and inorganic carbon losses by leaching, and $F_{harvest}$ is the carbon export through harvest. See Loubet et al. (2011) for details. We limited the carbon balance study to the 2006–2010 period published in Loubet et al. (2011). Indeed, computing the full period 2005–2019 carbon balance requires filling a year gap in 2018 and processing the leaching flux, which implies crop and leaching modelling, as well as an uncertainty analysis that goes beyond the scope of this manuscript.

3 Results

3.1 Summary statistics of soil properties

Statistical analysis confirmed a significant decompaction from 2005 to 2019, evidenced by a reduction in bulk density, particularly in the 0–5 cm ($p < 0.001$) and 5–30 cm ($p < 0.001$) layers (**Figure 3, Table S5**). BD decreased by ~25% in the 0–5 cm layer and by ~5% in the 5–30 cm layer, while the 30–60 cm layer presented a slight but non-significant increase. Similar results were observed for the fine earth density (Table S4). For the entire 0–60 cm profile, the average soil stock (FE_{0-60cm}) in 2005 was 882.5 kg m^{-2} , which was **approximately** 5% greater than in 2019 (840.1 kg m^{-2}). **Meanwhile**, the soil mass in the 0–5 cm layer decreased by **about** 25%. The SOC contents varied from 2005 to 2019 (**Figure 3, Table S5**). In the 0–5 cm layer, SOC contents were significantly higher in 2019 than in 2005 by around $2.2 \pm 0.57 \text{ g C kg}^{-1}$ ($p = 0.002$). In contrast, SOC content in the 5–30 cm layer was significantly lower by 6.2% in 2019 compared to 2005, with a mean difference of $-1.14 \pm 0.28 \text{ g C kg}^{-1}$ ($p < 0.001$). In the 30–60 cm layer, SOC contents remained statistically unchanged $-0.14 \pm 0.31 \text{ g C kg}^{-1}$, $p = 0.66$).

393



394

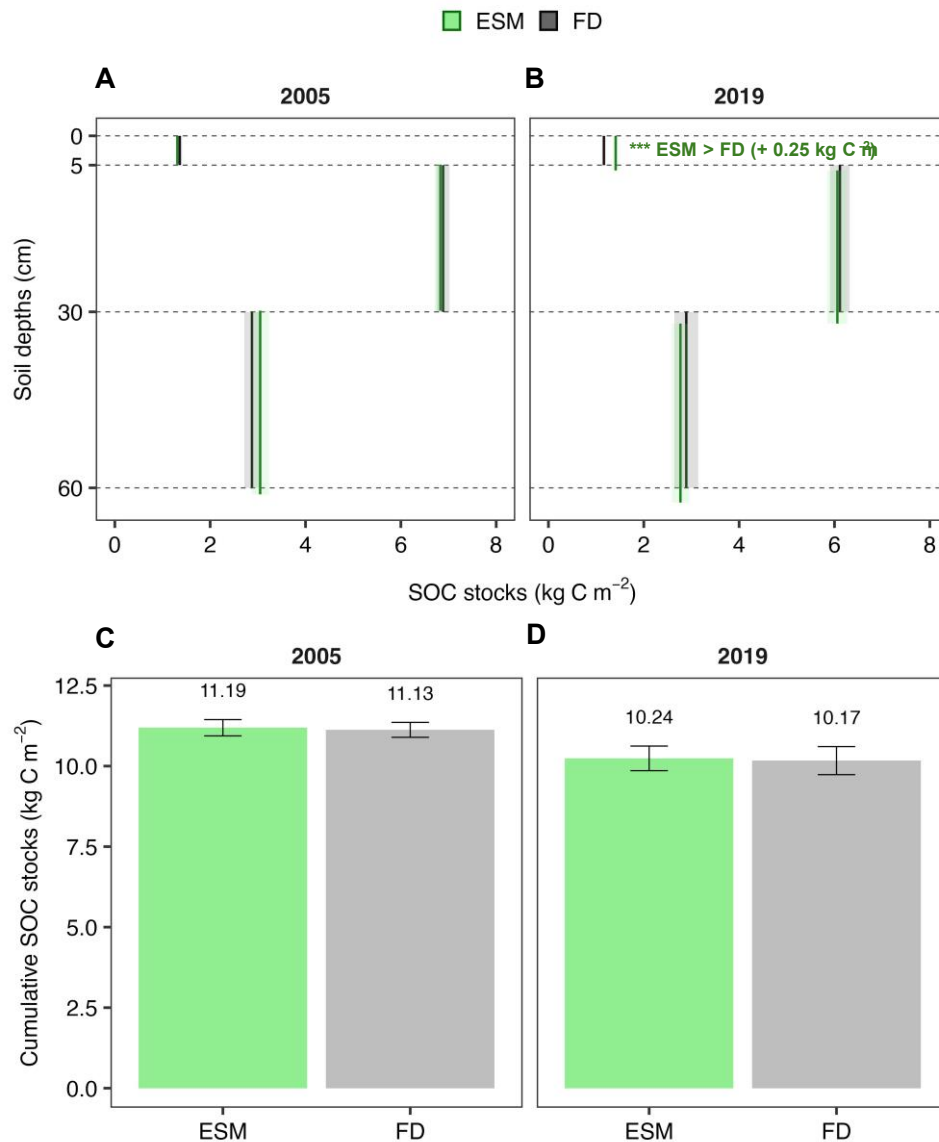
395 **Figure 3.** Mean of bulk density, soil organic carbon (SOC) contents, and **ESM-based SOC** stocks with their correspond-
396 **ing** confidence intervals (CIs) in the 2005 and 2019 campaigns across three soil layers (0-5, 5-30, 30-60 cm). **Mind that**
397 **the layer depths given here do not correspond to absolute depths since the ESM method implies varying depths with**
398 **time. The real depths corresponding to these layers are shown in Figure 5B.**

399

400 3.2 Differences between FD and ESM-based SOC stocks

401 **The** FD and ESM approaches were statistically similar in 2005 across the three soil layers (Figure 4A) **and only**
402 **showed** significant differences in the **0-5 cm** soil layer in 2019 (Figure 4B). **Both** approaches did not differ when
403 comparing the cumulative SOC stocks up to ~60 cm (all $p > 0.5$, Figure 4C-D).

404



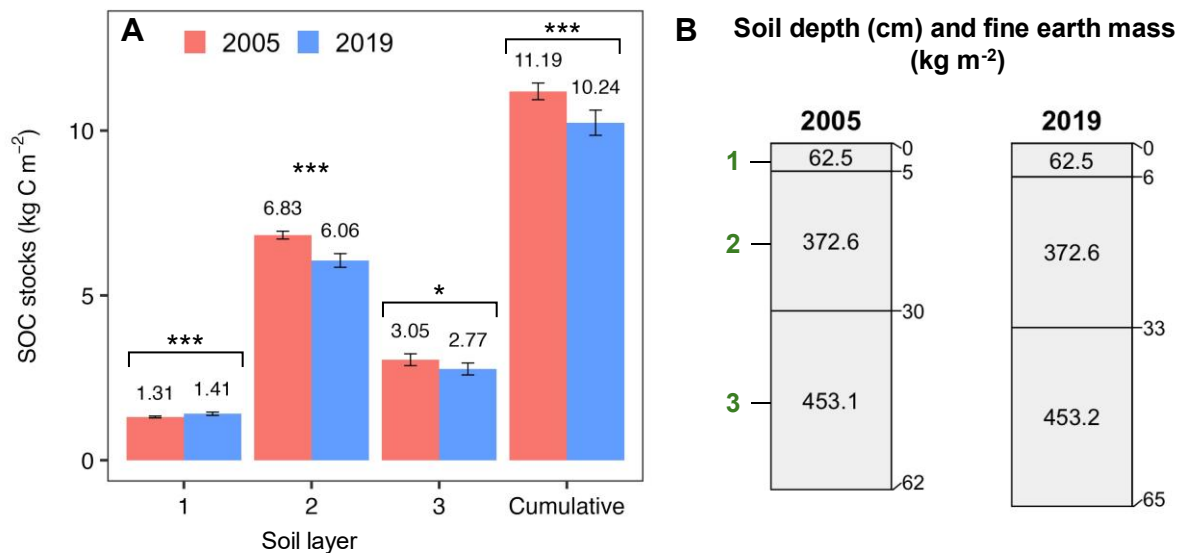
405
 406 **Figure 4.** Soil Organic Carbon stocks and corresponding confidence intervals (error bars and shaded ribbons) estimated
 407 using Fixed Depth (FD) and Equivalent Soil Mass (ESM) approaches. **Panels A and B** show SOC stocks per depth range
 408 for 2005 and 2019. Solid lines (vertical) represent mean SOC stocks across the entire depth range. Dashed horizontal
 409 grey lines represent the fixed soil depth layers, aggregated into 0-5 cm, 5-30 cm, and 30-60 cm. If the thickness of the
 410 ESM-adjusted depth falls outside the upper or lower bounds of the fixed soil depth, it indicates that a depth adjustment
 411 was made during the ESM computation. **Panels C and D** show cumulative SOC stocks over the 0-60 cm layer for 2005
 412 and 2019. Asterisks denote significant differences between SOC stock estimation methods ($P < 0.001$ corresponds
 413 to ***).

414

415 3.3 Soil carbon stock changes over time

416 The mass-equivalent depth (**Figure 5B**) varied **between years** according to the reference soil mass shown in **Table**
 417 **2**. On average, the mass-equivalent depths in 2019 were 0-6 cm, 6-33 cm, and 33-65 cm. In 2005, the soil depth
 418 adjustment was minimal compared to the sampling depth, with an increase of 2 ± 0.7 cm in the third layer (30-62
 419 cm). The ESM estimates indicated a **cumulative loss of soil organic carbon over the three layers**
 420 **of -0.95 ± 0.20 kg C m⁻² between 2005 and 2019 (Figure 5A)**. In the 0-5 cm layer, a higher SOC stock was

421 **measured in 2019 compared to 2005 (+0.10 ± 0.02 kg C m⁻²)**. The second layer (sampling depth of 5–30 cm)
 422 showed a lower SOC stock in 2019, with a **SOC stock change** of about **0.8 ± 0.10 kg C m⁻²**. In the deeper layer
 423 (sampling depth of 30–60 cm), SOC stock changes showed a **less significant** reduction of about **0.28 ± 0.11 kg**
 424 **C m⁻²**. Effect-size comparisons between the two campaigns across the three layers **confirmed the significance of**
 425 **the SOC changes between 2005 and 2019 (Figure S8)**. **A finer vertical analysis (Figure S9) indicates that the**
 426 **SOC stocks in 2019 were higher in the layer L1 (~0-5 cm), then decreased between layers L3 and L5 (~20 and**
 427 **~40 cm), before increasing again in layers L6 and L7 (~ 40 - 60 cm).**
 428



429
 430 **Figure 5. Mean soil organic carbon (SOC) stocks (kg C m⁻²) estimated using the Equivalent Soil Mass (ESM), along**
 431 **with their corresponding confidence intervals (error bars), for the 2005 and 2019 campaigns (Panel A).** Adjusted soil
 432 **depth (cm) and fine earth mass (kg m⁻²) are also shown in Panel B.** Asterisks denote significant differences between
 433 **campaigns: $P < 0.001$ (***) , $P < 0.01$ (**), $P < 0.05$ (*).**
 434

435 3.4 Cumulative SOC stocks

436 Across the 13.25-year monitoring period, the cumulative SOC stocks up to the sampling fixed depth of 0-60 cm
 437 exhibited a statistically significant decline ($p < 0.05$) of **approximately** **0.95 ± 0.22 kg C m⁻²** ($p < 0.001$; MDD <
 438 observed differences, **Table 3**). A similar decline was found using the ESM and the FD. Overall, both SOC esti-
 439 mation approaches indicate an average SOC loss of approximately **72 ± 16 g C m⁻² yr⁻¹** over the 13.25-year period.
 440 In terms of proportional reduction relative to the 2005 baseline, ESM-based SOC stocks decreased by **-8.2%** in
 441 the **~0–30 cm** layer and **-8.5%** in the **~0–60 cm** layer. These losses translate to annualised losses of approximately
 442 **-0.62% to -0.89% yr⁻¹**, when referenced to the 2005 SOC stocks baseline.

443 **Table 3. Summary of soil organic carbon (SOC) stock changes between 2005 and 2019 in the “Reduced field” at the FR-**
 444 **Gri site, assessed for the 0–30 cm and 0–60 cm soil layers using both the Equivalent Soil Mass (ESM) and Fixed-Depth**
 445 **(FD) approaches. SOC changes are reported in absolute terms (kg C m⁻²) followed by their standard error, relative**
 446 **change (% of initial stock), and as annualised rates. The Minimum Detectable Difference (MDD) represents the smallest**
 447 **true difference that can be statistically detected given the observed variability and sample size. If the observed SOC**
 448 **stock change exceeds the MDD and $p < 0.05$, the change is considered detectable. If the SOC stock change is less than**
 449 **the MDD, the change is not statistically distinguishable. A large MDD reflects high variability or limited sensitivity,**
 450 **whereas a small MDD indicates high precision in detecting changes in SOC stock. These estimates were also used as**
 451 **input parameters for the AMG model simulations.**

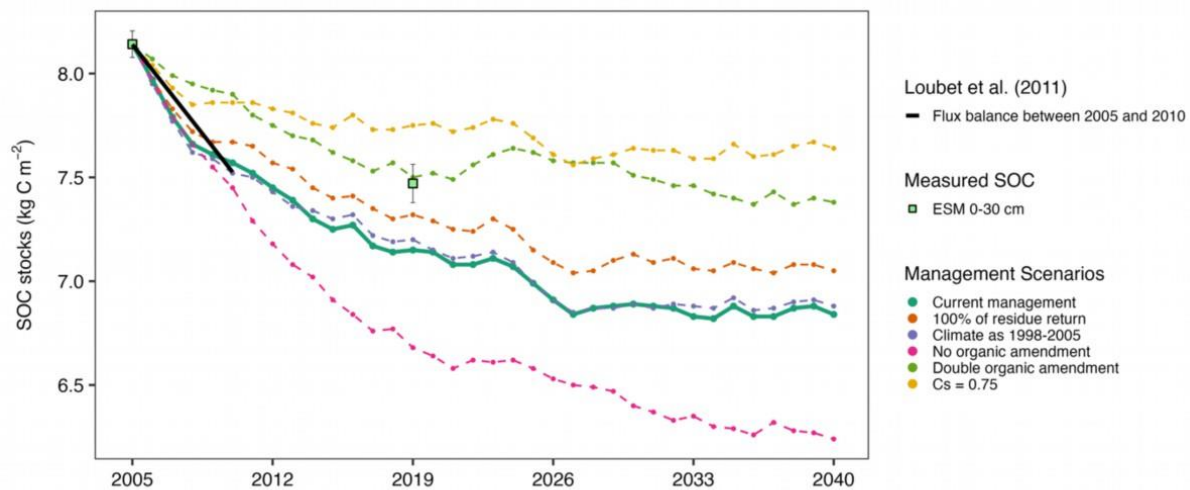
Metric	Equivalent Soil Mass		Fixed depth	
	~ 0-30 cm * 435.1 kg m ⁻²	~ 0-60 cm 887.6 kg m ⁻²	0-30 cm *	0-60 cm
2005 SOC stocks (kg C m ⁻²)	8.14 ± 0.06	11.19 ± 0.13	8.25 ± 0.08	11.12 ± 0.12
2019 SOC stocks (kg C m ⁻²)	7.47 ± 0.09	10.24 ± 0.16	7.28 ± 0.09	10.17 ± 0.18
SOC stock change (kg C m ⁻²)	-0.67	-0.95	-0.97	-0.96
Standard Error difference (kg C m ⁻²)	0.11	0.04	0.12	0.04
Lower CI difference (kg C m ⁻²)	-0.90	-1.37	-1.22	-1.40
Upper CI difference (kg C m ⁻²)	-0.44	-0.53	-0.72	-0.51
<i>P values</i> (two-sided)	< 0.001	< 0.001	< 0.001	< 0.001
Minimum Detectable Difference (kg C m ⁻²)	0.38	0.71	0.41	0.76
SOC stock change (% of initial Stock)	-8.2%	-8.5%	-11.8%	-8.6%
SOC stock change (% initial Stock yr ⁻¹)	-0.62% yr ⁻¹	-0.65% yr ⁻¹	-0.89% yr ⁻¹	-0.64% yr ⁻¹
SOC stock change (per mil initial Stock yr ⁻¹)	-6.2‰ yr ⁻¹	-6.5‰ yr ⁻¹	-8.9‰ yr ⁻¹	-6.4‰ yr ⁻¹

* SOC stocks from 2005 at 0-30 and 0-60 cm were inserted as input variables in the AMG model.

452
453
454

455 3.5 Comparison of measured SOC stock changes with estimations obtained with the AMG model

456 The AMG model was used to simulate the **evolution of** soil organic carbon stock from 2005 to 2040 in the 0-30
 457 cm layer, based on the cropping system, imports and exports, **and** computing the **return of** plant residues **using**
 458 allometric relationships. Under **the baseline scenario**, the model **exhibited** a declining trend **in** SOC stocks (Fig-
 459 ure 6), which aligns with the decrease observed **using** the ESM approach in the 0-30 cm layer. **The AMG model**
 460 **simulated a decrease in SOC stock** from 8.24 kg C m⁻² in 2005 to 7.25 kg C m⁻² in 2019, reflecting a cumulative
 461 loss of approximately -0.99 kg C m⁻² (-12%) over 13.25 years. **This modelled SOC loss is larger than the mean**
 462 **SOC stock change estimated using the ESM approach in the 0-30 cm layer (-0.67 kg C m⁻²), and slightly**
 463 **outside the associated confidence intervals (95% CI: -0.90 to -0.44 kg C m⁻²; Table 3). SOC stocks appear to**
 464 approach a quasi-steady-state from 2027 onwards, with fluctuations of ±0.02 to ±0.04 kg C m⁻² yr⁻¹. By 2040, SOC
 465 stocks are projected to decrease to 6.94 kg C m⁻², representing an approximate 15% reduction from the 2005 base-
 466 line. Both the AMG model and measured SOC stocks were consistent with the flux balance approach reported by
 467 Loubet et al. (2011), during the early period from 2006 to 2010. The overall loss over 22 **years** (2005-2027) would
 468 then be of around 1.3 kg C m⁻², or 13 Mg C ha⁻¹, which amounts to 0.059 Mg ha⁻¹ yr⁻¹. Overall, the sensitivity
 469 analysis across five scenarios **reveals a consistent decline** in SOC, with cumulative losses ranging from 5 to 18%
 470 by 2019 and from 6 to 23% by 2040. Increasing the residue return leads to a stabilisation of the SOC stock **at** 7.15
 471 **kg C m⁻²**, instead of 6.95 kg C m⁻², while doubling the organic carbon amendment would lead to an equilibrium
 472 of 7.48 kg C m⁻². On the contrary, suppressing the organic carbon amendment would lead to a stabilisation of 6.34
 473 kg C m⁻². **The simulation with a climate corresponding to 1998-2005 (slightly colder, with a temperature of**
 474 **-0.3°C compared to 2005-2019) had no detectable effect on the simulated soil C stock (Figure 6).**



475
476
477 **Figure 6. Soil organic carbon (SOC) stock in the 0-30 cm depth as simulated by the AMG model (plot lines), measured**
478 **by soil sampling in 2005 and 2019 and computed using the equivalent soil mass (ESM; light-green square). The error**
479 **bars show the sampling standard error. Flux balance over the 2006-2010 period (black line) as published in Loubet et**
480 **al. (2011). Cs denotes the proportion of stable carbon pools in the model.**

481 4 Discussion

482 4.1 Effects of sampling depth and computation methods on the evaluation of organic carbon stock 483 changes evaluation

484 Our results show that cumulative SOC stock changes between 2005 and 2019 under reduced tillage management
485 were similar between the FD and ESM approaches only when SOC stocks were integrated over the complete
486 0–60 cm profile, differing by just 3% in this layer ($p > 0.80$). In contrast, SOC stock changes differed between
487 approaches in the surface soil (≤ 30 cm). Previous studies have documented misleading interpretations of SOC
488 stock increases resulting from reduced or no-tillage practices when using the FD approach at shallow depths
489 (≤ 30 cm) (Du et al., 2017; Xiao et al., 2020). Our results support this in the 0-5 cm layer, where FD indicates SOC
490 stock losses while ESM shows gain (Table S5, Figure S8). Indeed, FD approaches are prone to bias when soil
491 bulk density or SOC content changes, irrespective of the soil management (von Haden et al., 2020). Because BD
492 often varies with management in agricultural soils, especially at shallow depths (≤ 30 cm), multilayer sampling
493 and equivalent soil mass approaches are essential to capture the temporal response of SOC stock in shallow layers
494 (Wendt and Hauser, 2013; Xiao et al., 2020). At the FR-Gri site, the topsoil (0–15 cm) is frequently disturbed by
495 shallow tillage using a stubble cultivator or clod crusher, and deep tillage operations have occasionally been ap-
496 plied to depths of up to 40 cm. In addition to residue return, these practices influence BD and soil mass distribution,
497 particularly within the upper 40 cm of the profile. Additionally, the potential compaction caused by repeated ma-
498 chinery traffic cannot be excluded (Hamza and Anderson, 2005), as compaction tends to accumulate over time
499 below 40 cm due to the limited tillage operations in the subsoil (Zhang et al., 2024). Roots may also alter BD,
500 including in subsurface layers, by modifying the physical properties (e.g., aggregation, porosity) as roots effi-
501 ciently explore deeper layers. At the FR-Gri site, we observe a significant decrease in BD in the 0-5 cm and 5-30
502 cm layers, with no significant change in the lower layer (30-60 cm) (Table S4). Likewise, roots may contribute to
503 subsoil SOC stocks through root growth, biomass accumulation, and rhizodeposition. The rhizodeposition process
504 may account for up to 65% of root carbon (C) and ~10% of total photosynthesised carbon, as shown for maize

505 (Tardieu, 1988) and wheat (Zhang et al., 2020; Zou et al., 2022), **which are** the main crops at the FR-Gri site. Fan
506 et al. (2016) reported that approximately 95% of root biomass lies above 100 cm. In our field, 20% of the SOC
507 stock changes occurred in the 30-60 cm layer, confirming that sampling to at least 60 cm better captures root-
508 related C inputs and reduces SOC bias estimate, as also emphasised by Baker et al. (2007) and Wendt and Hauser
509 (2013). Furthermore, SOC stock estimates in **more profound** and multiple layers provide valuable insights into
510 SOC dynamics across the profile, as mineralised carbon may percolate and accumulate in subsoil layers (Rumpel
511 and Kögel-Knabner, 2011).

512 **4.2 Possible causes of the observed SOC stock changes over 13.25 years**

513 SOC stock losses in cropland systems under various management practices have been widely reported in European
514 studies (De Rosa et al., 2024). A major cause of carbon losses is the imbalance between carbon imports and ex-
515 ports, which progressively leads to a shift in the carbon stock from one state to a new one, higher if the imbalance
516 is an excess of imports or lower in the opposite case (Ingwersen et al., 2024; Poyda et al., 2019). Over the 13.25-
517 year period (2005–2019), the FR-Gri site has experienced a decrease in SOC stock of 0.95 kg C m^{-2} [95% CI: 0.51-
518 1.4]. Our study **has** evidenced that C losses in the intermediate soil layers (**5-40 cm**) are not offset by gains **below**,
519 down to **a depth of approximately** 60 cm (~0-5 and 40-60 cm). **Overall**, the **cropping system history** at FR-Gri
520 **resulted in** a carbon stock decrease of $72 \pm 16 \text{ g C m}^{-2} \text{ yr}^{-1}$ over the **observed 13.25-year period** in the ~0-60
521 cm soil layer, irrespective of the SOC estimation method. **We hypothesise** that SOC decline is primarily related
522 to **an imbalance during that period** between carbon imports, limited by reduced crop residue return, and high
523 biomass exports. The FR-Gri site has been under continuous cropland management for over 100 years, with re-
524 duced tillage and crop rotation introduced in the past two decades. In the 1980s, the field received an unquantified
525 but **significant** amount of organic matter inputs from wastewater treatment plants, **which may explain the high**
526 **carbon stocks observed in 2005**. Moreover, since 2004, **the** increased export of wheat straw for bioenergy has
527 reduced crop residue **returns**, while **the use of** organic amendments **has been** limited (Table 1). This shift in
528 management practices may have contributed to a long-term imbalance between C imports and exports, leading to
529 SOC stock declines, **as** the field exports were, **on average**, around **three times** higher than imports and twice
530 higher than the **combined** import and aerial residue return. The AMG simulations corroborate this hypothesis,
531 showing a decrease **primarily attributed to** the low residue return and limited organic C application. **At the same**
532 **time, the slight shift in meteorological conditions** ($+0.3 \text{ }^\circ\text{C}$ air temperature) **during that** period **has no** signif-
533 icant effect on the **simulated** soil C stock (**Figure 6**).

534 **Different patterns have been reported in long-term experiments conducted under similar pedoclimatic con-**
535 **ditions. In a well-drained Haplic Luvisol under a temperate climate, Dimassi et al. (2014) demonstrated that**
536 **changes in SOC stock under residue removal varied over time, exhibiting alternating phases of accumula-**
537 **tion and depletion. The most substantial depletion occurred around 2002 ($-0.033 \text{ kg C m}^{-2} \text{ yr}^{-1}$), possibly**
538 **reflecting the lagged effects of residue removal between 1982 and 1994, as well as the impact of climate**
539 **change. In contrast, the SOC stock increased in 2011 after residues were returned after 1994. Furthermore,**
540 **SOC stocks increased in the upper soil layer (0-10 cm) but were offset by losses at depth (10-28 cm), resulting**
541 **in near-neutral changes in SOC stock over the profile. These trends were later confirmed by Mary et al.**
542 **(2020), who conducted additional sampling in 2017. Unlike the long-term experiments of Dimassi et al.**
543 **(2014) and Mary et al. (2020), where surface gains largely compensated subsoil losses at the profile scale,**

544 **SOC losses at FR-Gri were dominated by sustained carbon deficits in intermediate layers, resulting in a net**
545 **negative balance. However, as we hypothesised here, Dimassi et al. (2014) suggested that crop management**
546 **practices, such as residue removal, crop rotation (C3 vs. C4), and catch crops, mediate C sequestration**
547 **under similar soil tillage conditions.**

548 **The relatively high initial SOC stocks at FR-Gri reflect the previously high though unrecorded C inputs**
549 **(from wastewater treatment plants) and lower residue exports. This may further contribute to the observed**
550 **decline in SOC stock, as C inputs decreased during the 2005-2019 period, despite the presence of** substantial
551 organic inputs. In terms of soil processes, SOC stock declines during **this period likely** reflect an imbalance be-
552 tween SOC mineralization and **stabilization processes** rates, likely triggered by high fresh plant inputs with low
553 C: N ratio, organic amendments, nitrogen-rich fertilisation (193 kg N ha⁻¹) **and environmental conditions fa-**
554 **vouring microbial activity and SOC mineralisation** (Bernard et al., 2022; Ceschia et al., 2010; Loubet et al.,
555 **201). The depleting effect of nitrogen-rich inputs** was also observed **by Dimassi et al. (2014), who found that**
556 **SOC was depleted under a crop rotation without a C4 plant and increased after the establishment of a catch**
557 **crop (oats/vetch).**

558 Keel et al. (2019) reported ESM-based SOC stock losses ranging from 0.01 to 0.135 kg C m⁻² yr⁻¹ across various
559 crop systems in Switzerland, with an average loss of 0.034 kg C m⁻² yr⁻¹ in the topsoil (~0–20 cm). Their highest
560 SOC stock losses were observed under a crop rotation similar to that of FR-Gri, with a comparable initial stock
561 (~7 kg C m⁻² in the 0–20 cm layer), but implemented on an Orthic Luvisol. We notice that their C inputs from
562 residue return and organic fertilisation (0.090–0.32 kg C m⁻² yr⁻¹) are comparable to ours (0.265 ± 0.030 kg C m⁻²).
563 **Still,** they attributed the C losses to the recent **conversion of** grassland (with high SOC stock) to cropland (with
564 low SOC stock), which may explain the doubled carbon stock change compared to this study.

565 The AMG model **reproduced the** observed SOC stock **decline**, though with a **slightly greater magnitude, rein-**
566 **forcing the conclusion** that the **FR-Gri soil was** not in carbon equilibrium and that **a persistent negative C**
567 **balance** is the most plausible **driver of SOC losses during that period** (Figure 6). **The model projections sug-**
568 **gest** that the SOC stock should **decline** at the same rate until 2027 **before stabilising**. A sensitivity analysis **reveals**
569 that increasing the residue return would lead to a stabilisation of the SOC stock **at 7.2 kg C m⁻², compared to**
570 **6.95 kg C m⁻² under current management**, while doubling the organic carbon amendment would **result in** an
571 equilibrium of 7.5 kg C m⁻². **Conversely,** suppressing organic carbon **amendments**, which may be **close to** reality
572 with the installation of a biogas plant on the farm, would lead to a stabilisation of 6.3 kg C m⁻². **Although** not
573 explicitly simulated in our study, digestate residues from biogas production could serve as an alternative organic
574 amendment. While this residue typically contains lower content of labile organic carbon compared to fresh organic
575 material, the remaining organic material tends to be more chemically recalcitrant and resistant to microbial de-
576 composition. As a result, their incorporation **into** the soil may contribute to slight but persistent increases in SOC
577 stocks over time (Keel et al., 2025; Thomsen et al., 2013).

578 **Finally, the** integrated carbon fluxes from 2006 to 2010 (Loubet et al., 2011) confirm a carbon loss from the soil
579 **comparable to that simulated by** the AMG model (Figure 6). Although the uncertainties **in** the integrated carbon
580 fluxes are **substantial**, the convergence between the two approaches corroborates a **significant** soil carbon loss in
581 the years 2005-2010, which is consistent with the **decrease in** organic carbon **fertilisation** and residue return
582 during that period (Table 1) **compared to previous years**. We also note that the yearly carbon loss from Loubet
583 et al. (2011) is not significantly different from the yearly carbon soil destocking found in the present study. In the

584 north-western part of Switzerland, in a Cambisol soil, Leifeld et al. (2011) compared integrated carbon fluxes and
585 soil sampling methods over 5 years on **both** an intensive and an extensive grassland **that had been** recently con-
586 verted from intensive cropland. They concluded that the **significant** uncertainties in both methods prevented **the**
587 **detection of** a significant change over 5 years in the intensive field. On the contrary, in the extensive field, they
588 found a significant decrease of the SOC stock of $-0.217 \pm 0.143 \text{ kg C m}^{-2} \text{ yr}^{-1}$ by soil sampling, but a lower loss of
589 $-0.065 \pm 0.092 \text{ g C m}^{-2} \text{ yr}^{-1}$ based on the integrated carbon fluxes method.

590 **4.3 Uncertainties in soil carbon stock changes**

591 We recognise the importance of distinguishing **an actual** SOC stock change from artefacts introduced by differ-
592 ences in sampling designs in 2005 and 2019. To address this, the clustering of the soil based on 2019 soil properties
593 (**See Supplementary Material and Methods, Figure S1**) provides an objective way to subset the 2019 dataset
594 **for comparison** with the 2005 campaign **under** similar soil **conditions**. The data-driven area selection corrobo-
595 rates the farmer's expert knowledge of the field heterogeneity. The robustness, across both design- and model-
596 based approaches, alongside the clustering of soil properties to identify distinct soil groups, increases our confi-
597 dence that the observed differences reflect **fundamental** changes in **soil carbon** stocks over time.

598 In the *Reduced field* (**Figure S4**), the observed SOC stock change between 2005 and 2019 in the 0-60 cm layer
599 was $-0.95 \pm 0.22 \text{ kg C m}^{-2}$, exceeding the minimum detectable difference (MDD) of 0.73 kg C m^{-2} ($p < 0.01$), and
600 this represents both significant and detectable changes given our sample size and design. In contrast, the *Complete*
601 *field* (**Figure S4**) did not **exhibit** the same pattern, as the observed SOC changes fell below the MDD, **suggesting**
602 that the changes detected between 2005 and 2019 **may have been** masked by spatial heterogeneity. **For these**
603 **reasons, computations** using the Complete field **were not** considered **in this study, as they could lead to a** Type
604 II error (failing to detect a real effect). The larger MDD when all strata are included in our comparisons reflect
605 increased soil heterogeneity, particularly related to the potential presence of Calcisol (shallow soil with high rock
606 fragments and SIC content) on the north-western part of the field. These factors not only affect the soil bulk density
607 and fine earth mass, but also the **soil's capacity to stabilise** carbon through positive interactions between Calcium
608 (Ca) and soil organic matter (Kleber et al., 2021). **These factors also lead to significant variability in biomass**
609 **production, with the Calcisol area, which retains less water, being less productive, as observed by harvest**
610 **maps (Loubet et al., 2011). This leads to fewer carbon inputs in this area through the return of residues to**
611 **the soil.**

612 Additional uncertainty on the overall SOC stock change at the site may come from inorganic carbon losses. Indeed,
613 previous measurements of carbon leaching at the FR-Gri site indicated that inorganic carbon, whose stock change
614 could not be evaluated with the 2005 sampling data, may also contribute to significant soil carbon losses. Kindler
615 et al. (2011) showed that, in 2010, the site was losing $28 \text{ g C m}^{-2} \text{ yr}^{-1}$ through leaching with a contribution of
616 $21 \text{ g C m}^{-2} \text{ yr}^{-1}$ as dissolved inorganic carbon (DIC). Inorganic carbon leaching dominates at the site, with 75% of
617 the leached **carbon** being inorganic, indicating **an apparent** dissociation **of carbonates** to DIC leaching due to
618 H^+ . Although not measured directly as a soil stock change, we can therefore evaluate that carbonate leaching would
619 lead to an additional inorganic soil carbon loss of $21 \text{ g C m}^{-2} \text{ yr}^{-1}$, leading to a total of $72 + 21 = 93 \text{ g C m}^{-2} \text{ yr}^{-1}$
620 carbon loss. The inorganic carbon loss would therefore represent a very significant amount of 22% of the total
621 carbon lost from the field, which could be induced by high nitrogen fertilisation (193 kg N ha^{-1} as half organic,
622 half mineral, Table 1) and base cations exports by harvest (Raza et al., 2021; Song et al., 2022; Zamanian et al.,

2021). We should, however, bear in mind that even if C is lost by DIC-DOC leaching from the 0-60 cm layer, it may lead to a deep C sequestration by formation of secondary CaCO₃ (An et al., 2019; Liu et al., 2022).

Based on the uncertainties identified in this study, several key points should be considered for the next resampling campaign to enhance the detectability of stock changes in SOC. First, maintaining consistency in the sampled area and sampling protocols (including material used for sampling) across campaigns is critical to avoid confounding temporal changes with spatial variability. Second, sampling depth should also extend sufficiently deep (1 m) as SOC losses and gains vary across the soil profile. Third, accurate quantification of bulk density, rock fragment content, and fine earth mass remains essential, and consistent protocols should be applied across campaigns to ensure compatibility with equivalent soil mass approaches. Finally, Consistent recording of meteorology, carbon fluxes, and C inputs and outputs, together with their uncertainties, is also key to interpreting the observations. The application of the ICOS harmonised protocols fulfils all the above-mentioned key points and ensures methodological consistency and comparability across years, particularly when using equivalent soil mass approaches. Some additional observations that are not mandatory in ICOS may be beneficial for further understanding soil carbon stock changes, particularly in terms of organic and inorganic carbon leaching. Together, these considerations will enhance the ability of future resampling campaigns to detect SOC stock changes robustly and distinguish between management and environmental-driven effects, as well as spatial and methodological sources of uncertainty.

5 Conclusions

A significant decompaction of the 0-5 cm soil layer was observed over the 13.25 years in this crop field, with an estimated 22% decrease in bulk density in the 0-5 cm layer and a 5% decrease in the 5-30 cm layer. This decompaction is likely due to reduced deep tilling and increased intercropping since 2004. However, despite the higher SOC content in 2019, SOC stocks increased **only** in the 0-5 cm layer, **while decreasing** in the 5-30 cm layer, with no **change** in the 30-60 cm layer. Consequently, cumulative SOC stocks in the 0-60 cm layer decreased by $0.95 \pm 0.22 \text{ kg C m}^{-2}$, as estimated by the equivalent soil mass approach. As we observed a similar decrease when using a fixed depth approach in the 0-60 cm layer, we conclude that sampling at a depth of 60 cm in agricultural soils is a good way to minimise biases in soil carbon stock evolution estimates.

The annual decrease of cumulative SOC stock was $72 \pm 16 \text{ g C m}^{-2} \text{ yr}^{-1}$, equivalent to a $-0.65\% \text{ yr}^{-1}$ rate of decline. This rate is consistent with earlier studies and supported by the AMG model simulation and flux balance approach over the 2005-2010 period for our site. Our study, therefore, suggests that reduced tillage, intercropping, and organic fertilisation may not be sufficient to prevent soil carbon losses when the initial SOC stock is high, as in our site. As confirmed by other studies, the losses observed here highlight the difficulty of achieving the 4-per-mille aspirational target in cropping systems representative of the Parisian Basin, which are characterised by relatively large SOC stocks and **significant** exports.

While our study detected changes **in SOC stock** between 2005 and 2019, **substantial** uncertainties remain. Notably, the shift from a regular-grid design in 2005 (N = 100, nested within the 2019 footprint) to a stratified random design in 2019 (N = 20 covering the entire C-flux footprint) may introduce artefacts related to soil heterogeneity and reduced statistical power. This calls for additional campaigns in the future with the same sampling design as in 2019. According to the AMG model runs, a change of around 0.3 kg C m^{-2} is expected between 2019 and 2028,

661 which would be just above the standard error difference of 0.22 kg C m⁻² found here, indicating that a sample in
662 2028 would be meaningful.

663 These uncertainties call for standardised, high-quality monitoring protocols such as those developed by the ICOS
664 research infrastructure. Consistent sampling methodologies over time are needed to reliably assess the long-term
665 impact of crop management on SOC stocks at sites like FR-Gri, and to improve our understanding of carbon
666 dynamics in cropland systems. Integrating SOC stock data with CO₂ flux measurements **and lateral carbon fluxes**
667 will be crucial to exploring the underlying processes driving SOC changes.

668 **Acknowledgements**

669 We acknowledge the AgroParisTech Grignon farm and its director, Dominique Tristant, for letting us access their
670 field and providing information on practices and yields, the direction of the infrastructure of INRAE for funding
671 the ICOS FR-Gri site, and EU projects CarboEurope, NitroEurope and ECLAIRE for funding this work. Data
672 processing, including the sample analysis, was supported by the ICOS Ecosystem Thematic Centre. G.N. acknowl-
673 edges Horizon Europe funding (Open-Earth-Monitor Cyberinfrastructure project, 101059548). D.P. thanks the
674 support of the ITINERIS Project (IR0000032 - CUP B53C22002150006) funded under the EU - Next Generation
675 EU Mission 4. B.W. thanks the support of the exploratory research program FairCarboN funded by the Agence
676 Nationale de la Recherche under the France 2030 program, reference ANR-22-PEXF-0002 – **project** ALAMOD.
677 We greatly acknowledge Marion Schrumpf from the Max Planck Institute and her team for sharing the 2005 soil
678 sampling data. We also thank Eric Larmanou for helping in the field during the soil sampling campaign in 2005.

679 **Code/Data availability**

680 The **Level-2 data from the** 2019 campaign are **publicly available through** the ICOS **Carbon Portal** (Buysse et
681 al., 2025). The **raw data from both sampling campaigns, all input files (including the complete R project),**
682 **and the R scripts used for data processing and analysis are available in Winck et al. (2026).**

683 **Authors contribution**

684 BL conceptualised, supervised, acquired the funding for the study and administered the project. BL and MG co-
685 wrote the original draft of the manuscript with contributions from all co-authors and revised it. NS and BW pro-
686 vided the formal analysis, provided the statistical expertise and scripts to compute the carbon stocks in the original
687 manuscript, and co-wrote the manuscript. PB made the soil sampling and data curation for the 2019 campaign,
688 curated the crop management data and reviewed the manuscript. JPC and NS participated in the ICOS database
689 data curation. CD managed the soils storage in 2019, contributed to data curation, and reviewed the manuscript.
690 CJ provided expertise on the soil sampling methodology. CK made data curation on the crop management data
691 and reviewed the manuscript. FL computed the AMG and reviewed the manuscript. BW and JLME provided
692 expertise on the ESM methodology and reviewed the manuscript. SL participated in data curation and reviewed
693 the manuscript. DL and DP conceptualised the data acquisition and reviewed the manuscript. GN participated in
694 the data curation. DA initiated the project, conceptualised, developed and provided expertise on the methodology
695 and revised the manuscript.

6 References

- An, H., Wu, X., Zhang, Y., and Tang, Z.: Effects of land-use change on soil inorganic carbon: A meta-analysis, *Geoderma*, 353, 273–282, <https://doi.org/https://doi.org/10.1016/j.geoderma.2019.07.008>, 2019.
- 700 Antón, R., Arricibita, F. J., Ruiz-Sagasetta, A., Enrique, A., de Soto, I., Orcaray, L., Zaragüeta, A., and Virto, I.: Soil organic carbon monitoring to assess agricultural climate change adaptation practices in Navarre, Spain, *Reg Environ Change*, 21, <https://doi.org/10.1007/s10113-021-01788-w>, 2021.
- Arrouays, D., Saby, N. P. A., Boukir, H., Jolivet, C., and Rati: Soil sampling and preparation for monitoring soil carbon, *Int Agrophys*, 32, 633–643, <https://doi.org/10.1515/intag-2017-0047>, 2018.
- 705 Aubinet, M., Moureaux, C., Bodson, B., Dufranne, D., Heinesch, B., Suleau, M., Vancutsem, F., and Vilret, A.: Carbon sequestration by a crop over a 4-year sugar beet/winter wheat/seed potato/winter wheat rotation cycle, *Agric For Meteorol*, 149, 407–418, <https://doi.org/10.1016/j.agrformet.2008.09.003>, 2009.
- Autret, B., Mary, B., Chenu, C., Balabane, M., Girardin, C., Bertrand, M., Grandeau, G., and Beaudoin, N.: Alternative arable cropping systems: A key to increase soil organic carbon storage? Results from a 16 year field
710 experiment, *Agric Ecosyst Environ*, 232, 150–164, <https://doi.org/10.1016/j.agee.2016.07.008>, 2016.
- Baker, J. M., Ochsner, T. E., Venterea, R. T., and Griffis, T. J.: Tillage and soil carbon sequestration - What do we really know?, *Agric Ecosyst Environ*, 118, 1–5, <https://doi.org/10.1016/j.agee.2006.05.014>, 2007.
- Batjes, N. H.: Total carbon and nitrogen in the soils of the world, *Eur J Soil Sci*, 47, 151–163, <https://doi.org/DOI.10.1111/j.1365-2389.1996.tb01386.x>, 1996.
- 715 Baveye, P. C., Berthelin, J., Tessier, D., and Lemaire, G.: The “4 per 1000” initiative: A credibility issue for the soil science community?, *Geoderma*, 309, 118–123, <https://doi.org/https://doi.org/10.1016/j.geoderma.2017.05.005>, 2018.
- Beem-Miller, J. P., Kong, A. Y. Y., Ogle, S., and Wolfe, D.: Sampling for Soil Carbon Stock Assessment in Rocky Agricultural Soils, *Soil Science Society of America Journal*, 80, 1411–1423, <https://doi.org/10.2136/sssaj2015.11.0405>, 2016.
- 720 Bernard, L., Basile-Doelsch, I., Derrien, D., Fanin, N., Fontaine, S., Guenet, B., Karimi, B., Marsden, C., and Maron, P.: Advancing the mechanistic understanding of the priming effect on soil organic matter mineralisation, *Funct Ecol*, 36, 1355–1377, <https://doi.org/10.1111/1365-2435.14038>, 2022.
- Brisson, N., Mary, B., Ripoche, D., Jeuffroy, M. H., Ruget, F., Nicoullaud, B., Gate, P., Devienne-Barret, F.,
725 Antonioletti, R., Durr, C., Richard, G., Beaudoin, N., Recous, S., Tayot, X., Plenet, D., Cellier, P., Mchet, J.-M., Meynard, J. M., and Delécolle, R.: STICS: a generic model for the simulation of crops and their water and nitrogen balances. I. Theory and parameterization applied to wheat and corn, *Agronomie*, 18, 311–346, <https://doi.org/10.1051/agro:19980501>, 1998.
- Brown, A. L.: Design Experiments: Theoretical and Methodological Challenges in Creating Complex Interventions in Classroom Settings, *Journal of the Learning Sciences*, 2, 141–178, https://doi.org/10.1207/s15327809jls0202_2, 1992.
- 730 Brus, D. J. and deGrujter, J. J.: Random sampling or geostatistical modelling? Choosing between design-based and model-based sampling strategies for soil (with discussion), *Geoderma*, 80, 1–44, [https://doi.org/10.1016/s0016-7061\(97\)00072-4](https://doi.org/10.1016/s0016-7061(97)00072-4), 1997.

- 735 Brus, D. J. and Saby, N. P. A.: Approximating the variance of estimated means for systematic random sampling, illustrated with data of the French Soil Monitoring Network, *Geoderma*, 279, 77–86, <https://doi.org/10.1016/j.geoderma.2016.05.016>, 2016.
- Buysse, P., Loubet, B., Depuydt, J., Durand, B., and Kalalian, C.: ETC L2 ARCHIVE from Grignon, 2021–2025, <https://hdl.handle.net/11676/gEj9nfPY-ImTffWmZmjCmxg4>, 2025.
- 740 Canty, A., Ripley, B., and Brazzale, A. R.: Package “boot”, <https://doi.org/10.32614/CRAN.package.boot>, 2024.
- Ceschia, E., Béziat, P., Dejoux, J. F., Aubinet, M., Bernhofer, C., Bodson, B., Buchmann, N., Carrara, A., Cellier, P., Di Tommasi, P., Elbers, J. A., Eugster, W., Grünwald, T., Jacobs, C. M. J., Jans, W. W. P., Jones, M., Kutsch, W., Lanigan, G., Magliulo, E., Marloie, O., Moors, E. J., Moureaux, C., Olioso, A., Osborne, B., Sanz, M. J., Saunders, M., Smith, P., Soegaard, H., and Wattenbach, M.: Management effects on net ecosystem carbon and GHG budgets at European crop sites, *Agric Ecosyst Environ*, 139, 363–383, <https://doi.org/10.1016/j.agee.2010.09.020>, 2010.
- 745 Chen, L., Liu, L., Qin, S., Yang, G., Fang, K., Zhu, B., Kuzyakov, Y., Chen, P., Xu, Y., and Yang, Y.: Regulation of priming effect by soil organic matter stability over a broad geographic scale, *Nat Commun*, 10, <https://doi.org/10.1038/s41467-019-13119-z>, 2019.
- 750 Chenu, C., Angers, D. A., Barré, P., Derrien, D., Arrouays, D., and Balesdent, J.: Increasing organic stocks in agricultural soils: Knowledge gaps and potential innovations, *Soil Tillage Res*, 188, 41–52, <https://doi.org/https://doi.org/10.1016/j.still.2018.04.011>, 2019.
- Clivot, H., Mouny, J.-C., Duparque, A., Dinh, J.-L., Denoroy, P., Houot, S., Vertès, F., Trochard, R., Bouthier, A., Sagot, S., and Mary, B.: Modeling soil organic carbon evolution in long-term arable experiments with AMG model, *Environmental Modelling & Software*, 118, 99–113, <https://doi.org/https://doi.org/10.1016/j.envsoft.2019.04.004>, 2019.
- 755 Clivot, H., Duparque, A., Ferchaud, F., Lagrange, H., Levvasseur, F., Levert, M., Marsac, S., Mary, B., Mouny, J.-C., Piquemal, B., Sagot, S., Servain, F., Trochard, R., Cadoux, S., and Perrin, A.-S.: AMGv2 parameters, <https://doi.org/https://doi.org/10.57745/MEQQIX>, 7 June 2023.
- 760 Coleman, K. and Jenkinson, D. S.: RothC-26.3 - A Model for the turnover of carbon in soil, in: *Evaluation of Soil Organic Matter Models*, Springer Berlin Heidelberg, Berlin, Heidelberg, 237–246, https://doi.org/10.1007/978-3-642-61094-3_17, 1996.
- Collins, A.: Toward a Design Science of Education, in: *New Directions in Educational Technology*, edited by: Scanlon, E. and O’Shea, T., Springer Berlin Heidelberg, Berlin, Heidelberg, 15–22, https://doi.org/10.1007/978-3-642-77750-9_2, 1992.
- 765 Corti, G., Ugolini, F. C., and Agnelli, A.: Classing the Soil Skeleton (Greater than Two Millimeters): Proposed Approach and Procedure, *Soil Science Society of America Journal*, 62, 1620–1629, <https://doi.org/https://doi.org/10.2136/sssaj1998.03615995006200060020x>, 1998.
- De Rosa, D., Ballabio, C., Lugato, E., Fasiolo, M., Jones, A., and Panagos, P.: Soil organic carbon stocks in European croplands and grasslands: How much have we lost in the past decade?, *Glob Chang Biol*, 30, <https://doi.org/10.1111/gcb.16992>, 2024.
- 770 Dimassi, B., Mary, B., Wylleman, R., Labreuche, J. Ô., Couture, D., Piraux, F., and Cohan, J. P.: Long-term effect of contrasted tillage and crop management on soil carbon dynamics during 41 years, *Agric Ecosyst Environ*, 188, 134–146, <https://doi.org/10.1016/j.agee.2014.02.014>, 2014.

- 775 Don, A., Schumacher, J., Scherer-Lorenzen, M., Scholten, T., and Schulze, E.-D.: Spatial and vertical variation of soil carbon at two grassland sites — Implications for measuring soil carbon stocks, *Geoderma*, 141, 272–282, <https://doi.org/https://doi.org/10.1016/j.geoderma.2007.06.003>, 2007.
- Du, Z., Angers, D. A., Ren, T., Zhang, Q., and Li, G.: The effect of no-till on organic C storage in Chinese soils should not be overemphasized: A meta-analysis, *Agric Ecosyst Environ*, 236, 1–11, <https://doi.org/https://doi.org/10.1016/j.agee.2016.11.007>, 2017.
- 780 Efron, B.: Better Bootstrap Confidence Intervals, *J Am Stat Assoc*, 82, 171–185, <https://doi.org/10.1080/01621459.1987.10478410>, 1987.
- Ellert, B. H. and Bettany, J. R.: Calculation of organic matter and nutrients stored in soils under contrasting management regimes, *Can J Soil Sci*, 75, 529–538, <https://doi.org/10.4141/cjss95-075>, 1995.
- 785 Fan, J., McConkey, B., Wang, H., and Janzen, H.: Root distribution by depth for temperate agricultural crops, *Field Crops Res*, 189, 68–74, <https://doi.org/10.1016/j.fcr.2016.02.013>, 2016.
- FAO: Measuring and modelling soil carbon stocks and stock changes in livestock production systems: Guidelines for assessment, Versuib 1., Livestock Environmental Assessment and Performance (LEAP) Partnership, Rome, 170 pp., 2019.
- 790 Ferchaud, F., Chlebowski, F., and Mary, B.: SimpleESM: R script to calculate soil organic carbon and nitrogen stocks at Equivalent Soil Mass, 1–9 pp., 2023.
- Franzluebbers, A. J., Paine, L. K., Winsten, J. R., Krome, M., Sanderson, M. A., Ogles, K., and Thompson, D.: Well-managed grazing systems: A forgotten hero of conservation, *J Soil Water Conserv*, 67, <https://doi.org/10.2489/jswc.67.4.100A>, 2012.
- 795 Goovaerts, P.: *Geostatistics for natural resources evaluation*, Oxford University Press, New York, 0–483 pp., <https://doi.org/https://doi.org/10.1023/A:1007530422454>, 1997.
- Gräler, B., Pebesma, E., and Heuvelink, G.: Spatio-Temporal Interpolation using *gstat*, *R J*, 8, 204, <https://doi.org/10.32614/RJ-2016-014>, 2016.
- de Gruijter, J. J., Bierkens, M. F. P., Brus, D. J., and Knotters, M.: *Sampling for Natural Resource Monitoring*, Springer Berlin Heidelberg, Berlin, Heidelberg, 334 pp., <https://doi.org/10.1007/3-540-33161-1>, 2006.
- 800 von Haden, A. C., Yang, W. H., and DeLucia, E. H.: Soils’ dirty little secret: Depth-based comparisons can be inadequate for quantifying changes in soil organic carbon and other mineral soil properties, *Glob Chang Biol*, 26, 3759–3770, <https://doi.org/10.1111/gcb.15124>, 2020.
- Hamza, M. A. and Anderson, W. K.: Soil compaction in cropping systems, *Soil Tillage Res*, 82, 121–145, <https://doi.org/10.1016/j.still.2004.08.009>, 2005.
- 805 Harbo, L. S., Olesen, J. E., Liang, Z., Christensen, B. T., and Elsgaard, L.: Estimating organic carbon stocks of mineral soils in Denmark: Impact of bulk density and content of rock fragments, *Geoderma Regional*, 30, e00560, <https://doi.org/https://doi.org/10.1016/j.geodrs.2022.e00560>, 2022.
- Hedges, L. V.: Distribution theory for Glass’s estimator of effect size and related estimators, *Journal of Educational Statistics*, 6, 107–128, <https://doi.org/10.2307/1164588>, 1981.
- 810 Heiskanen, J., Brummer, C., Buchmann, N., Calfapietra, C., Chen, H., Gielen, B., Gkritzalis, T., Hammer, S., Hartman, S., Herbst, M., Janssens, I. A., Jordan, A., Juurola, E., Karstens, U., Kasurinen, V., Kruijt, B., Lankreijer, H., Levin, I., Linderson, M. L., Loustau, D., Merbold, L., Myhre, C. L., Papale, D., Pavelka, M., Pilegaard, K., Ramonet, M., Reibmann, C., Rinne, J., Rivier, L., Saltikoff, E., Sanders, R., Steinbacher,

- 815 M., Steinhoff, T., Watson, A., Vermeulen, A. T., Vesala, T., Vítková, G., and Kutsch, W.: The Integrated Carbon Observation System in Europe, *Bull Am Meteorol Soc*, 103, E855–E872, <https://doi.org/10.1175/BAMS-D-19-0364.1>, 2022.
- Hijmans, R. J.: raster: Geographic Data Analysis and Modeling, <https://doi.org/10.32614/CRAN.package.raster>, 20 March 2010.
- 820 Hopkins, D. W., Waite, I. S., McNicol, J. W., Poulton, P. R., Macdonald, A. J., and O'Donnell, A. G.: Soil organic carbon contents in long-term experimental grassland plots in the UK (Palace Leas and Park Grass) have not changed consistently in recent decades, *Glob Chang Biol*, 15, 1739–1754, <https://doi.org/10.1111/j.1365-2486.2008.01809.x>, 2009.
- Ingwersen, J., Poyda, A., Kremer, P., and Streck, T.: Harvest residues: A relevant term in the carbon balance of croplands?, *Agric For Meteorol*, 349, <https://doi.org/10.1016/j.agrformet.2024.109935>, 2024.
- 825 IPCC: Generic methodologies applicable to multiple land-use categories, Refinement to the 2006 IPCC guidelines, 2019.
- Kanari, E., Cécillon, L., Baudin, F., Clivot, H., Ferchaud, F., Houot, S., Levvasseur, F., Mary, B., Soucémariadin, L., Chenu, C., and Barré, P.: A robust initialization method for accurate soil organic carbon simulations, *Biogeosciences*, 19, 375–387, <https://doi.org/10.5194/bg-19-375-2022>, 2022.
- 830 Keel, S. G., Anken, T., Büchi, L., Chervet, A., Fliessbach, A., Flisch, R., Huguenin-Elie, O., Mäder, P., Mayer, J., Sinaj, S., Sturny, W., Wüst-Galley, C., Zihlmann, U., and Leifeld, J.: Loss of soil organic carbon in Swiss long-term agricultural experiments over a wide range of management practices, *Agric Ecosyst Environ*, 286, <https://doi.org/10.1016/j.agee.2019.106654>, 2019.
- 835 Keel, S. G., Budai, A., Elsgaard, L., Hardy, B., Levvasseur, F., Zhi, L., Mondini, C., Plaza, C., and Leifeld, J.: Efficiency of Plant Biomass Processing Pathways for Long-Term Soil Carbon Storage, *Eur J Soil Sci*, 76, <https://doi.org/10.1111/ejss.70074>, 2025.
- Kindler, R., Siemens, J., Kaiser, K., Walmsley, D. C., Bernhofer, C., Buchmann, N., Cellier, P., Eugster, W., Gleixner, G., Grunwald, T., Heim, A., Ibrom, A., Jones, S. K., Jones, M., Klumpp, K., Kutsch, W., Larsen, 840 K. S., Lehuger, S., Loubet, B., McKenzie, R., Moors, E., Osborne, B., Pilegaard, K., Reibmann, C., Saunders, M., Schmidt, M. W. I., Schrumpf, M., Seyfferth, J., Skiba, U., Soussana, J. F., Sutton, M. A., Tefs, C., Vowinkel, B., Zeeman, M. J., and Kaupenjohann, M.: Dissolved carbon leaching from soil is a crucial component of the net ecosystem carbon balance, *Glob Chang Biol*, 17, 1167–1185, <https://doi.org/10.1111/j.1365-2486.2010.02282.x>, 2011.
- 845 Kirby, K. N. and Gerlanc, D.: BootES: An R package for bootstrap confidence intervals on effect sizes, *Behav Res Methods*, 45, 905–927, <https://doi.org/10.3758/s13428-013-0330-5>, 2013.
- Kleber, M., Bourg, I. C., Coward, E. K., Hansel, C. M., Myneni, S. C. B., and Nunan, N.: Dynamic interactions at the mineral–organic matter interface, <https://doi.org/10.1038/s43017-021-00162-y>, 11 May 2021.
- Kljun, N., Calanca, P., Rotach, M. W., and Schmid, H. P.: A Simple Parameterisation for Flux Footprint Predictions, *Boundary Layer Meteorol*, 112, 503–523, <https://doi.org/10.1023/B:BOUN.0000030653.71031.96>, 850 2004.
- Kljun, N., Calanca, P., Rotach, M. W., and Schmid, H. P.: A simple two-dimensional parameterisation for Flux Footprint Prediction (FFP), *Geosci. Model Dev.*, 8, 3695–3713, <https://doi.org/10.5194/gmd-8-3695-2015>, 2015.

- 855 Knotters, M., Teuling, K., Reijneveld, A., Lesschen, J. P., and Kuikman, P.: Changes in organic matter contents and carbon stocks in Dutch soils, 1998–2018, *Geoderma*, 414, <https://doi.org/10.1016/j.geoderma.2022.115751>, 2022.
- Krauss, M., Wiesmeier, M., Don, A., Cuperus, F., Gattinger, A., Gruber, S., Haagsma, W. K., Peigné, J., Palazzoli, M. C., Schulz, F., van der Heijden, M. G. A., Vincent-Caboud, L., Wittwer, R. A., Zikeli, S., and Steffens, 860 M.: Reduced tillage in organic farming affects soil organic carbon stocks in temperate Europe, *Soil Tillage Res*, 216, <https://doi.org/10.1016/j.still.2021.105262>, 2022.
- Lal, R.: Carbon emission from farm operations, *Environ Int*, 30, 981–990, <https://doi.org/10.1016/j.envint.2004.03.005>, 2004.
- Lee, J., Hopmans, J. W., Rolston, D. E., Baer, S. G., and Six, J.: Determining soil carbon stock changes: Simple 865 bulk density corrections fail, *Agric Ecosyst Environ*, 134, 251–256, <https://doi.org/10.1016/j.agee.2009.07.006>, 2009.
- Liebhart, G., Toth, M., Stumpp, C., Bodner, G., Klik, A., Zhang, X., Strohmeier, S., and Strauss, P.: Developing topsoil structure through conservation management to protect subsoil from compaction, *Soil Tillage Res*, 253, 106669, <https://doi.org/10.1016/j.still.2025.106669>, 2025.
- 870 Lipiec, J. and Hatano, R.: Quantification of compaction effects on soil physical properties and crop growth, *Geoderma*, 116, 107–136, [https://doi.org/10.1016/S0016-7061\(03\)00097-1](https://doi.org/10.1016/S0016-7061(03)00097-1), 2003.
- Liu, J., Wu, P., Zhao, Z., and Gao, Y.: Afforestation on cropland promotes pedogenic inorganic carbon accumulation in deep soil layers on the Chinese loess plateau, *Plant Soil*, 478, 597–612, <https://doi.org/10.1007/s11104-022-05494-2>, 2022.
- 875 Loubet, B., Laville, P., Lehuger, S., Larmanou, E., Fléchar, C., Mascher, N., Genermont, S., Roche, R., Ferrara, R. M., Stella, P., Personne, E., Durand, B., Decuq, C., Flura, D., Masson, S., Fanucci, O., Rampon, J. N., Siemens, J., Kindler, R., Gabrielle, B., Schrumpf, M., and Cellier, P.: Carbon, nitrogen and Greenhouse gases budgets over a four years crop rotation in northern France, *Plant Soil*, 343, 109–137, <https://doi.org/10.1007/s11104-011-0751-9>, 2011.
- 880 Loustau, D., Jolivet, C., Lafont, S., Loubet, B., Klumpp, K., Papale, D., and Arrouays, D.: ICOS Ecosystem Instructions for Soil Samples Collection and Preparation (Version 20230727), <https://doi.org/https://doi.org/10.18160/k3yc-td6h>, 2017.
- Lu, H., Li, S., Ma, M., Baskrikov, V., Chen, X., Ciais, P., Dai, Y., Ito, A., Ju, W., Lienert, S., Lombardozzi, D., Lu, X., Maignan, F., Nakhavali, M., Quine, T., Schindlbacher, A., Wang, J., Wang, Y., Wrlind, D., Zhang, 885 S., and Yuan, W.: Comparing machine learning-derived global estimates of soil respiration and its components with those from terrestrial ecosystem models, *Environmental Research Letters*, 16, <https://doi.org/10.1088/1748-9326/abf526>, 2021.
- MacQueen, J.: Some methods for classification and analysis of multivariate observations, in: *Proceedings of the Fifth Berkeley Symposium on Mathematical Statistics and Probability*, 666, 1967.
- 890 Mary, B., Clivot, H., Blaszczyk, N., Labreuche, J., and Ferchaud, F.: Soil carbon storage and mineralization rates are affected by carbon inputs rather than physical disturbance: Evidence from a 47-year tillage experiment, *Agric Ecosyst Environ*, 299, <https://doi.org/10.1016/j.agee.2020.106972>, 2020.

- McBratney, Alex. B. and Minasny, B.: Comment on “Determining soil carbon stock changes: Simple bulk density corrections fail” [Agric. Ecosyst. Environ. 134 (2009) 251–256], *Agric Ecosyst Environ*, 136, 185–186, 895
<https://doi.org/10.1016/j.agee.2009.12.010>, 2010.
- Minasny, B., Malone, B. P., McBratney, A. B., Angers, D. A., Arrouays, D., Chambers, A., Chaplot, V., Chen, Z.-S., Cheng, K., Das, B. S., Field, D. J., Gimona, A., Hedley, C. B., Hong, S. Y., Mandal, B., Marchant, B. P., Martin, M., McConkey, B. G., Mulder, V. L., O’Rourke, S., Richer-de-Forges, A. C., Odeh, I., Padarian, J., Paustian, K., Pan, G., Poggio, L., Savin, I., Stolbovoy, V., Stockmann, U., Sulaeman, Y., Tsui, C.-C., 900
 Vågen, T.-G., van Wesemael, B., and Winowiecki, L.: Soil carbon 4 per mille, *Geoderma*, 292, 59–86, <https://doi.org/https://doi.org/10.1016/j.geoderma.2017.01.002>, 2017.
- Molteni, F. and Corti, S.: Long-term fluctuations in the statistical properties of low-frequency variability: dynamical origin and predictability, *Quarterly Journal of the Royal Meteorological Society*, 124, 495–526, 1998.
- Parton, W. J., Hartman, M., Ojima, D., and Schimel, D.: DAYCENT and its land surface submodel: description and testing, *Glob Planet Change*, 19, 35–48, [https://doi.org/10.1016/S0921-8181\(98\)00040-X](https://doi.org/10.1016/S0921-8181(98)00040-X), 1998. 905
- Paustian, K., Lehmann, J., Ogle, S., Reay, D., Robertson, G. P., and Smith, P.: Climate-smart soils, <https://doi.org/10.1038/nature17174>, 6 April 2016.
- Pebesma, E.: Simple Features for R: Standardized Support for Spatial Vector Data, *R J*, 10, 439, <https://doi.org/10.32614/RJ-2018-009>, 2018.
- 910 Pebesma, E. and Bivand, R.: *Spatial Data Science*, Chapman and Hall/CRC, New York, <https://doi.org/10.1201/9780429459016>, 2023.
- Pebesma, E. J.: Multivariable geostatistics in S: the gstat package, *Comput Geosci*, 30, 683–691, <https://doi.org/10.1016/j.cageo.2004.03.012>, 2004.
- Peng, Y., Chahal, I., Hooker, D. C., and Van Eerd, L. L.: Comparison of equivalent soil mass approaches to estimate soil organic carbon stocks under long-term tillage, *Soil Tillage Res*, 238, 915
<https://doi.org/10.1016/j.still.2024.106021>, 2024.
- Petrescu, A. M. R., McGrath, M. J., Andrew, R. M., Peylin, P., Peters, G. P., Ciais, P., Broquet, G., Tubiello, F. N., Gerbig, C., Pongratz, J., Janssens-Maenhout, G., Grassi, G., Nabuurs, G. J., Regnier, P., Lauerwald, R., Kuhnert, M., Balkovič, J., Schelhaas, M. J., van der Gon, H. A. C. D., Solazzo, E., Qiu, C., Pilli, R., 920
 Konovalov, I. B., Houghton, R. A., Günther, D., Perugini, L., Crippa, M., Ganzenmüller, R., Luijkx, I. T., Smith, P., Munassar, S., Thompson, R. L., Conchedda, G., Monteil, G., Scholze, M., Karstens, U., Brockmann, P., and Dolman, A. J.: The consolidated European synthesis of **CO₂ emissions** and removals for the European Union and United Kingdom: 1990-2018, <https://doi.org/10.5194/essd-13-2363-2021>, 28 May 2021.
- 925 Poepflau, C. and Don, A.: Carbon sequestration in agricultural soils via cultivation of cover crops - A meta-analysis, *Agric Ecosyst Environ*, 200, 33–41, <https://doi.org/10.1016/j.agee.2014.10.024>, 2015.
- Poepflau, C., Vos, C., and Don, A.: Soil organic carbon stocks are systematically overestimated by misuse of the parameters bulk density and rock fragment content, *SOIL*, 3, 61–66, <https://doi.org/10.5194/soil-3-61-2017>, 2017.
- 930 Poyda, A., Wizemann, H.-D., Ingwersen, J., Eshonkulov, R., Högy, P., Demyan, M. S., Kremer, P., Wulfmeyer, V., and Streck, T.: Carbon fluxes and budgets of intensive crop rotations in two regional climates of southwest Germany, *Agric Ecosyst Environ*, 276, 31–46, <https://doi.org/10.1016/j.agee.2019.02.011>, 2019.

- R Core Team: A language and environment for statistical computing, <https://www.R-project.org/>, 2025.
- 935 Raza, S., Zamanian, K., Ullah, S., Kuzyakov, Y., Virto II, and Zhou, J. B.: Inorganic carbon losses by soil acidification jeopardize global efforts on carbon sequestration and climate change mitigation, *J Clean Prod*, 315, <https://doi.org/10.1016/j.jclepro.2021.128036>, 2021.
- Rovira, P., Sauras, T., Salgado, J., and Merino, A.: Towards sound comparisons of soil carbon stocks: A proposal based on the cumulative coordinates approach, *Catena (Amst)*, 133, 420–431, <https://doi.org/10.1016/j.catena.2015.05.020>, 2015.
- 940 Rumpel, C. and Kögel-Knabner, I.: Deep soil organic matter—a key but poorly understood component of terrestrial C cycle, *Plant Soil*, 338, 143–158, <https://doi.org/10.1007/s11104-010-0391-5>, 2011.
- Saby, N. P. A., Bellamy, P. H., Morvan, X., Arrouays, D., Jones, R. J. A., Verheijen, F. G. A., Kibblewhite, M. G., Verdoodt, A., Berenyiueges, J., Freudenschuss, A., and Simota, C.: Will European soil-monitoring networks be able to detect changes in topsoil organic carbon content?, *Glob Chang Biol*, 14, 2432–2442, <https://doi.org/10.1111/j.1365-2486.2008.01658.x>, 2008.
- 945 Sanderman, J., Hengl, T., and Fiske, G. J.: Soil carbon debt of 12,000 years of human land use, *Proceedings of the National Academy of Sciences*, 114, 9575–9580, <https://doi.org/doi:10.1073/pnas.1706103114>, 2017.
- Schmidt, M. W. I., Torn, M. S., Abiven, S., Dittmar, T., Guggenberger, G., Janssens, I. A., Kleber, M., Kögel-Knabner, I., Lehmann, J., Manning, D. A. C., Nannipieri, P., Rasse, D. P., Weiner, S., and Trumbore, S. E.: Persistence of soil organic matter as an ecosystem property, <https://doi.org/10.1038/nature10386>, 6 October 2011.
- Schrumpf, M., Schulze, E. D., Kaiser, K., and Schumacher, J.: How accurately can soil organic carbon stocks and stock changes be quantified by soil inventories?, *Biogeosciences*, 8, 1193–1212, <https://doi.org/10.5194/bg-8-1193-2011>, 2011.
- 955 Schulze, E. D., Luysaert, S., Ciais, P., Freibauer, A., Janssens, I. A., Soussana, J. F., Smith, P., Grace, J., Levin, I., Thiruchittampalam, B., Heimann, M., Dolman, A. J., Valentini, R., Bousquet, P., Peylin, P., Peters, W., Rödenbeck, C., Etiope, G., Vuichard, N., Wattenbach, M., Nabuurs, G. J., Poussi, Z., Nieschulze, J., and Gash, J. H.: Importance of methane and nitrous oxide for Europe’s terrestrial greenhouse-gas balance, *Nat Geosci*, 2, 842–850, <https://doi.org/10.1038/ngeo686>, 2009.
- 960 Shepard, D.: A two-dimensional interpolation function for irregularly-spaced data, in: *Proceedings of the 1968 23rd ACM national conference on -*, 517–524, <https://doi.org/10.1145/800186.810616>, 1968.
- Six, J., Conant, R. T., Paul, E. A., and Paustian, K.: Stabilization mechanisms of soil organic matter: Implications for C-saturation of soils, *Plant and Soil*, 155–176 pp., 2002.
- Skadell, L. E., Schneider, F., Gocke, M. I., Guigue, J., Amelung, W., Bauke, S. L., Hobley, E. U., Barkusky, D., Honermeier, B., Kögel-Knabner, I., Schmidhalter, U., Schweitzer, K., Seidel, S. J., Siebert, S., Sommer, M., Vaziritabar, Y., and Don, A.: Twenty percent of agricultural management effects on organic carbon stocks occur in subsoils – Results of ten long-term experiments, *Agric Ecosyst Environ*, 356, <https://doi.org/10.1016/j.agee.2023.108619>, 2023.
- 970 Soleilhavoup, M. and Crisan, M.: Enquête pratiques culturales en grandes cultures et prairies 2017 - Principaux résultats (Version modifiée), <https://agreste.agriculture.gouv.fr/agreste-web/disaron/Chd2009/detail/>, 2021.

- Song, X. D., Yang, F., Wu, H. Y., Zhang, J., Li, D. C., Liu, F., Zhao, Y. G., Yang, J. L., Ju, B., Cai, C. F., Huang, B. A., Long, H. Y., Lu, Y., Sui, Y. Y., Wang, Q. B., Wu, K. N., Zhang, F. R., Zhang, M. K., Shi, Z., Ma, W. Z., Xin, G., Qi, Z. P., Chang, Q. R., Ci, E., Yuan, D. G., Zhang, Y. Z., Bai, J. P., Chen, J. Y., Chen, J., 975
Chen, Y. J., Dong, Y. Z., Han, C. L., Li, L., Liu, L. M., Pan, J. J., Song, F. P., Sun, F. J., Wang, D. F., Wang, T. W., Wei, X. H., Wu, H. Q., Zhao, X., Zhou, Q., and Zhang, G. L.: Significant loss of soil inorganic carbon at the continental scale, *Natl Sci Rev*, 9, <https://doi.org/10.1093/nsr/nwab120>, 2022.
- Tardieu, F.: Analysis of the spatial variability of maize root density .1. Effect of wheel compaction on the spatial arrangement of roots, *Plant Soil*, 107, 259–266, <https://doi.org/10.1007/bf02370555>, 1988.
- 980 Tennekes, M.: tmap: Thematic maps in R, *J Stat Softw*, 84, <https://doi.org/10.18637/jss.v084.i06>, 2018.
- Thomsen, I. K., Olesen, J. E., Møller, H. B., Sørensen, P., and Christensen, B. T.: Carbon dynamics and retention in soil after anaerobic digestion of dairy cattle feed and faeces, *Soil Biol Biochem*, 58, 82–87, <https://doi.org/10.1016/j.soilbio.2012.11.006>, 2013.
- Thorndike, R. L.: Who Belongs in the Family?, *Psychometrika*, 18, 267–276, 985
<https://doi.org/10.1007/BF02289263>, 1953.
- VandenBygaart, A. J. and Angers, D. A.: Towards accurate measurements of soil organic carbon stock change in agroecosystems, *Can J Soil Sci*, 86, 465–471, <https://doi.org/10.4141/s05-106>, 2006.
- Walvoort, D. J. J., Brus, D. J., and de Gruijter, J. J.: An R package for spatial coverage sampling and random sampling from compact geographical strata by k-means, *Comput Geosci*, 36, 1261–1267, 990
<https://doi.org/https://doi.org/10.1016/j.cageo.2010.04.005>, 2010.
- Wendt, J. W. and Hauser, S.: An equivalent soil mass procedure for monitoring soil organic carbon in multiple soil layers, *Eur J Soil Sci*, 64, 58–65, <https://doi.org/10.1111/ejss.12002>, 2013.
- Wiesmeier, M., Sporlein, P., Geuss, U., Hangen, E., Haug, S., Reischl, A., Schilling, B., von Lutzow, M., and Kogel-Knabner, I.: Soil organic carbon stocks in southeast Germany (Bavaria) as affected by land use, soil 995
type and sampling depth, *Glob Chang Biol*, 18, 2233–2245, <https://doi.org/10.1111/j.1365-2486.2012.02699.x>, 2012.
- Winck, B., Loubet, B., Saby, N., Gebleh, M., Buysse, P., Chenu, J.-P., Ratié, C., Jolivet, C., Kalalian, C., Levavasseur, F., Munera-Echeverri, J.-L., Lafont, S., Loustau, D., Papale, D., Nicolini, G., and Arrouays, D.: Data and R code for the manuscript “Carbon soil stock change in an intensive crop field near Paris reveals significant carbon losses over a decade”, *Recherche Data Gouv*, <https://doi.org/10.57745/IDYYFV>, 2026.**
- Xiao, L., Zhou, S., Zhao, R., Greenwood, P., and Kuhn, N. J.: Evaluating soil organic carbon stock changes induced by no-tillage based on fixed depth and equivalent soil mass approaches, *Agric Ecosyst Environ*, 300, 106982, <https://doi.org/10.1016/j.agee.2020.106982>, 2020.
- 1005 Xu, L., He, N. P., Yu, G. R., Wen, D., Gao, Y., and He, H. L.: Differences in pedotransfer functions of bulk density lead to high uncertainty in soil organic carbon estimation at regional scales: Evidence from Chinese terrestrial ecosystems, *J Geophys Res Biogeosci*, 120, 1567–1575, <https://doi.org/10.1002/2015JG002929>, 2015.
- Zamanian, K., Zhou, J. B., and Kuzyakov, Y.: Soil carbonates: The unaccounted, irrecoverable carbon source, *Geoderma*, 384, <https://doi.org/10.1016/j.geoderma.2020.114817>, 2021.

- 1010 Zhang, B., Jia, Y., Fan, H., Guo, C., Fu, J., Li, S., Li, M., Liu, B., and Ma, R.: Soil compaction due to agricultural machinery impact: A systematic review, *Land Degrad Dev*, 35, 3256–3273, <https://doi.org/10.1002/ldr.5144>, 2024.
- Zhang, X. X., Whalley, P. A., Ashton, R. W., Evans, J., Hawkesford, M. J., Griffiths, S., Huang, Z. D., Zhou, H., Mooney, S. J., and Whalley, W. R.: A comparison between water uptake and root length density in winter wheat: effects of root density and rhizosphere properties, *Plant Soil*, 451, 345–356, <https://doi.org/10.1007/s11104-020-04530-3>, 2020.
- 1015 Zou, J., Ziegler, A. D., Chen, D., McNicol, G., Ciais, P., Jiang, X., Zheng, C., Wu, J., Wu, J., Lin, Z., He, X., Brown, L. E., Holden, J., Zhang, Z., Ramchunder, S. J., Chen, A., and Zeng, Z.: Rewetting global wetlands effectively reduces major greenhouse gas emissions, *Nat Geosci*, 15, 627–632, <https://doi.org/10.1038/s41561-022-00989-0>, 2022.
- 1020